

Superior colliculus projections drive dopamine neuron activity and movement but not value

Carli L. Poisson, PhD^{1,2,3}, Amy R. Wolff, PhD^{1,2}, Julianna Prohofsky^{1,2}, Cassandra Herubin^{1,2}, Madelyn Blake, and Benjamin T. Saunders PhD^{1,2}

¹ Department of Neuroscience, University of Minnesota

² Medical Discovery Team on Addiction, University of Minnesota

³ Graduate Program in Neuroscience, University of Minnesota



Correspondence: BTS (bts@umn.edu, saunderslab.com)

To navigate complex environments, animals must rapidly integrate sensory information and respond appropriately to gather rewards and avoid threats. It is well established that dopamine neurons in the ventral tegmental area (VTA) and substantia nigra pars compacta (SNC) are key for creating and maintaining associations between environmental stimuli (i.e., cues) and the outcomes they predict, through Pavlovian learning. However, it remains unclear how relevant sensory information is integrated into dopamine (DA) pathways to guide exploration and learning. The superior colliculus (SC) receives direct visual input, and is anatomically positioned as a relay for rapid sensory augmentation of dopamine neurons, which could underlie the formation of Pavlovian associations. Here, we characterize the anatomical organization and functional impact of SC projections to the VTA and SNC in rats. First, using anatomical tracing techniques, we show that neurons in the intermediate and deep layers of SC synapse densely throughout the ventral midbrain, interfacing directly with neurons projecting to the striatum and ventral pallidum. Using fiber photometry, we find that these SC projections excite both dopamine and GABA neurons in the VTA and dopamine neurons in the SNC *in vivo*. Despite this, cues predicting SC terminal stimulation did not reliably evoke behavior on their own in an optogenetic Pavlovian conditioning paradigm. Further, optogenetic activation of SC terminals in the VTA/SNC did not support primary reinforcement or produce place preference or avoidance. Instead, we find that stimulation of SC terminals in the VTA and SNC reliably evoked head turning behavior. This body reorientation increased in intensity with repeated stimulations, suggesting that strengthening this circuit could underlie sensorimotor learning related to exploration and attentional bias. Together our results show that collicular neurons contribute to cue-guided learning by controlling pose adjustments through interaction with dopamine systems.

INTRODUCTION

To make sense of complex environments, animals rely on sensory information (i.e., cues) that, through Pavlovian learning, comes to predict biologically-relevant events, including rewards and threats. It has been well established that the midbrain dopamine system is crucial for the creation (Handler et al., 2019; Tsai et al., 2009) and expression (Fischbach & Janak, 2019; van Zessen et al., 2021) of cue-evoked conditioned behaviors (Berke, 2018; Berridge & Robinson, 1998; Mohebi et al., 2019; Saunders et al., 2018; Sharpe et al., 2017; Wise, 2009; Wise & Jordan, 2021). Notably, dopamine neurons respond to visual cues at faster latencies than would be possible through the canonical visual cortical processing pathway (da Silva et al., 2018; Redgrave et al., 1999; Schultz, 2007), suggesting a direct route of sensory information transmission to dopaminergic regions (Redgrave & Gurney, 2006). Despite this, the mechanisms underlying sensory integration with dopamine circuits remain

poorly understood, and inputs providing rapid sensory augmentation have not been well characterized.

One candidate for providing direct sensory information is the superior colliculus (SC), as it receives direct retinal input and is key for navigating space (Ito & Feldheim, 2018; May, 2006) and shifting attention (Dean et al., 1989; Krauzlis et al., 2013). The SC has been shown to influence motor behaviors via encoding of choice (Steinmetz et al., 2019; Thomas et al., 2023) and rewards (Ikeda & Hikosaka, 2007). The intermediate and deep layers of the SC are thought to act as a saliency gate, filtering and routing the most relevant information about the environment to downstream regions (Basso et al., 2021; Bertram et al., 2014; Bromberg-Martin et al., 2010a; Cooper et al., 1998; Evans et al., 2018; Lovejoy & Krauzlis, 2010; Mysore & Knudsen, 2011; Redgrave & Gurney, 2006; Wang et al., 2020; White et al., 2017), and some neurons there directly project to neurons in the VTA and SNC (Coizet

et al., 2003; Comoli et al., 2003; Dawbarn & Pycock, 1982; May et al., 2009; McHaffie et al., 2006). In primates and rodents, SC is active during reward-related tasks (Viviani et al., 2020) and involved in appetitive Pavlovian conditioning to visual cues (Takakuwa et al., 2017). In anesthetized rats, visual stimuli activate deep layer SC neurons, which is necessary for rapid dopamine neuron activity modulation in the ventral midbrain (Comoli et al., 2003; Redgrave et al., 2010). Further, disinhibition of the SC, but not visual cortex, allows for dopamine neurons to be responsive to visual stimuli in anesthetized rodents (Dommett et al., 2005). Two recent studies suggest that SC neurons projecting specifically to the ventral midbrain are important for multiple forms of appetitive behavior (Huang et al., 2021; Solié et al., 2022).

Thus, neural the architecture for routing of sensory information to dopamine neurons via the SC is in place, but how this circuit functions in the context of cue-based learning, value assignment, and attention remains unclear (Bromberg-Martin et al., 2010a; Kaźmierczak & Nicola, 2022; Redgrave & Gurney, 2006). Here, we investigated how SC projections to the VTA/SNC impact dopamine neuron activity and subsequent motivated behaviors in awake, freely behaving rats. Using a combination of approaches, we find that SC neurons projecting to the ventral midbrain activate dopamine neurons and drive postural changes without creating conditioned behavior or producing valence representations. Our results highlight a brain circuit that is important for guiding movement to redirect attention, via interaction with classic learning systems.

RESULTS

Superior colliculus projections to the VTA and SNC

We first examined superior colliculus (SC) projections to the rat ventral midbrain, using three complementary approaches (Fig 1). Injection of an AAV coding for GFP into the SC resulted in general expression throughout the intermediate and deep layers. Terminals from these neurons were visible throughout the ventral midbrain, including the VTA and SNC (Fig 1A,C). We counterstained this tissue for TH, demonstrating intermingling of SC neuron fibers with dopamine neurons in both regions (Fig 1C). To verify that these SC projections make synapses in the VTA/SNC, we injected the SC with a virus coding for the expression of membrane-bound GFP and mRuby conjugated to synaptophysin (Fig 1D), a synaptic labeling protein (Beier et al., 2015). This resulted in strong GFP expression in the VTA/SNC, reflecting axon terminal membranes, adjacent to dense

mRuby puncta, indicative of synaptic connections with VTA/SNC neurons (Fig 1E-G). Finally, we examined the projection patterns of VTA/SNC neurons that receive monosynaptic input from neurons in the SC. To do this, we made use of the anterograde transsynaptic transport properties of AAV1 (Zingg et al., 2017). An AAV1 coding for cre recombinase was injected into the SC, along with the injection of a second AAV coding for cre-dependent expression of mCherry into the VTA or SNC (Fig 1H). This resulted in strong mCherry expression in neurons in the VTA and SNC (Fig 1I). Examination of forebrain regions showed strong mCherry expressing terminal fibers throughout the dorsal and ventral striatum and ventral pallidum (Fig 1J). Together these results build on previous findings (Huang et al., 2021; Redgrave, Coizet, Comoli, McHaffie, et al., 2010; Solié et al., 2022), demonstrating strong innervation of VTA/SNC by the SC, including to neurons projecting to the broader meso-striatal network.

Superior colliculus projections excite VTA/SNC dopamine neurons *in vivo*

Above we demonstrate that SC neurons project strongly to the VTA and SNC. These inputs are thought to be largely glutamatergic (Redgrave, Coizet, Comoli, McHaffie, et al., 2010; Z. Zhou et al., 2019), but the general impact of SC neuron activity on the ventral midbrain neurons *in vivo* is unknown. To explore this, we used a combination of fiber photometry and optogenetics. GCaMP8f was expressed in dopamine neurons in TH-cre rats, to record population-level dopamine neuron activity in the VTA and SNC (Fig 2A,B) during optogenetic activation of SC terminals expressing the red-shifted opsin ChrimsonR. We delivered brief unsignaled laser stimulation at 5 or 20 Hz, first examining the effect on dopamine neurons collapsed across all recording sites (Fig 2C-J). Stimulation at 5 Hz (Fig 2C) produced a large phasic burst in dopamine neuron activity, followed by a sustained elevation during the laser window (Fig 2D,E; one-sample t test peak $t(9)=5.29$, $p=.0005$; AUC $t(9)=6.19$, $p=.0002$). This response returned to baseline immediately following laser offset (Fig 2F; paired t test $t(9)=3.56$, $p=.0061$). Stimulation at 20 Hz (Fig 2G) produced a flatter sustained response during the whole laser window (Fig 2 H,I; one sample t test peak $t(9)=5.035$, $p=.001$; AUC $t(9)=2.546$, $p=.034$). This response was slower to return to baseline after laser offset (Fig 2J; paired t test $t(9)=.226$, $p=.827$).

We next split the data by stim-recording location, for placements in the VTA versus SNC (Fig 2K-R). This revealed slight differences in the pattern of activation. At 5 Hz stimulation, VTA dopamine neuron activity showed

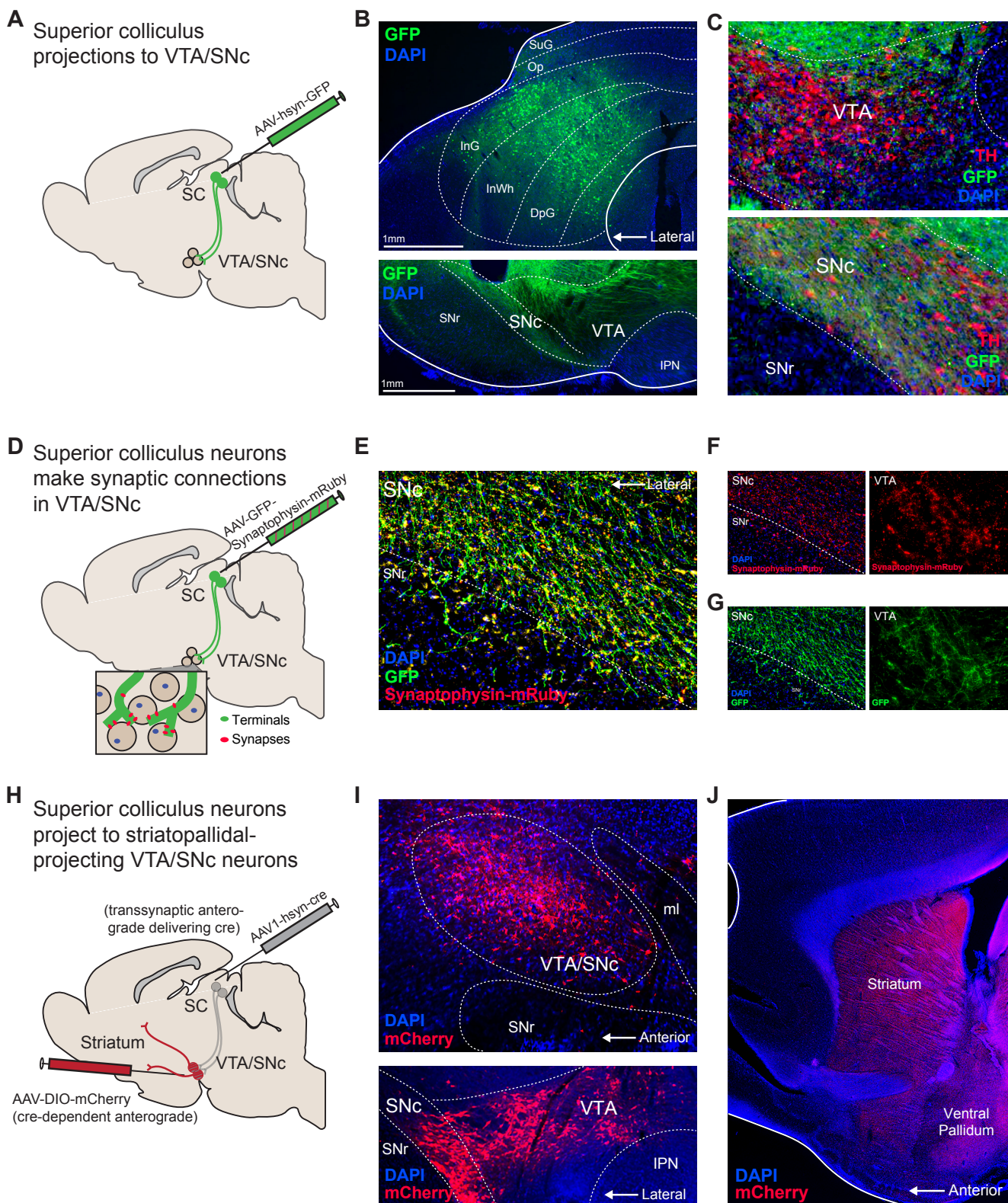


Fig 1. Superior colliculus projections to the ventral midbrain. A) Viral approach for targeting SC neurons. B) Injection of a GFP-expressing virus (green) into the SC resulted in expression throughout the intermediate and deep layers, with terminals visible throughout the ventral midbrain in the VTA and SNc. C) Tissue was counterstained for tyrosine hydroxylase (TH, red), demonstrating dense intermingling of SC projections with DA neurons in the VTA and SNc. D) Viral approach for visualizing monosynaptic connections between SC and the ventral midbrain. E) Injection of a virus coding for membrane-bound GFP and mRuby conjugated to the synaptophysin protein in the SC demonstrated strong innervation of the VTA and SNc. F) Dense mRuby puncta, indicating synaptic contacts between SC terminals and ventral midbrain neurons, were seen in VTA and SNc, G) closely associated with GFP-expressing terminals. H) Viral approach for transsynaptic tracing of SC-forebrain circuits. An AAV1 virus delivering cre recombinase was injected into the SC, combined with injection of a cre-dependent virus coding for mCherry into the VTA/SNc. I) Via the anterograde transsynaptic transport of AAV1-cre, we visualized VTA/SNc neurons receiving monosynaptic inputs from the SC (top: sagittal view; bottom: coronal view). J) mCherry fibers from VTA/SNc neurons receiving SC input were evident throughout the striatum and ventral pallidum in the forebrain.

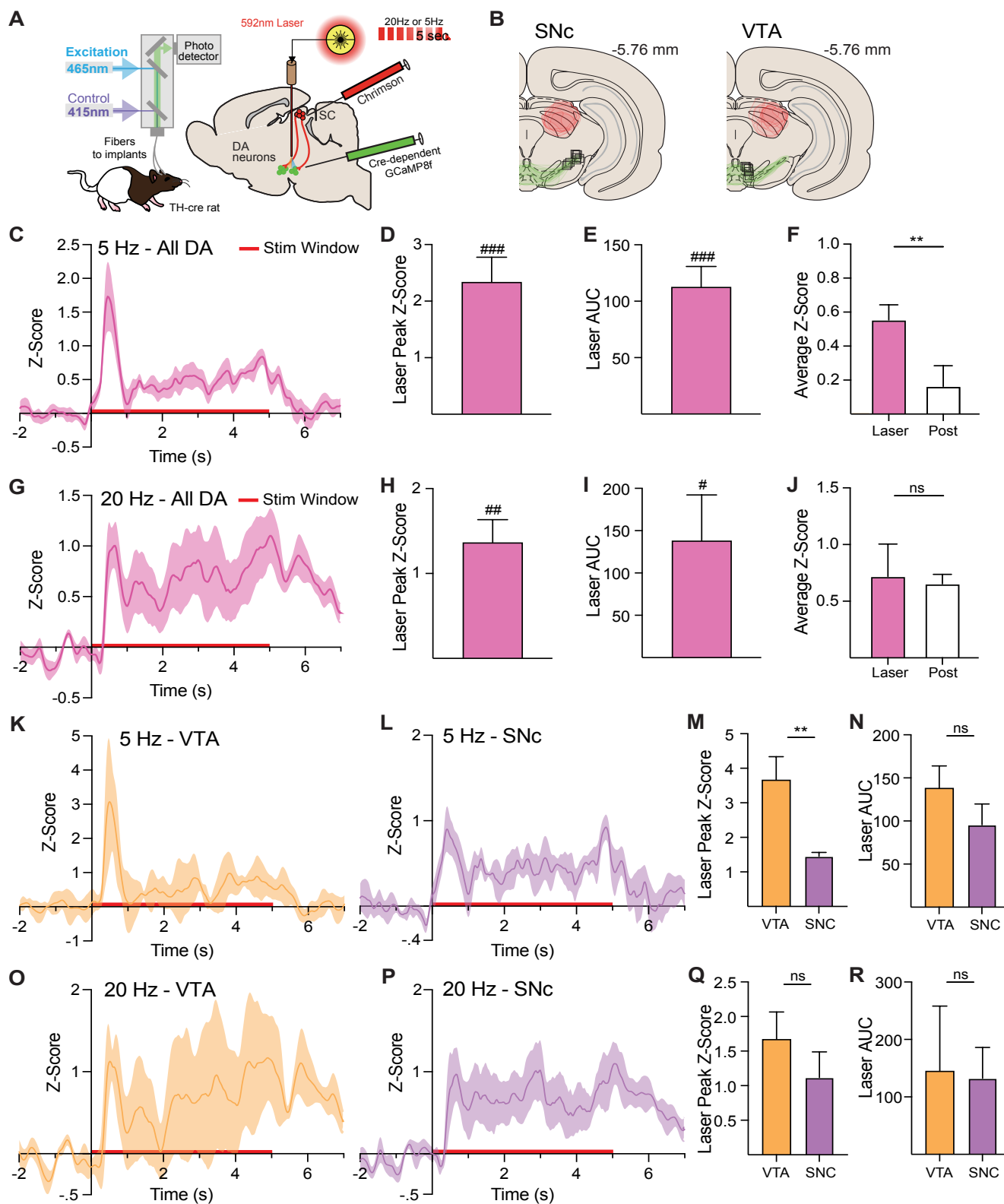


Fig 2. Superior colliculus projections activate dopamine neurons in the VTA and SNC in vivo. A) Approach to target SC terminals with the red-shifted excitatory opsin ChrimsonR and dopamine neurons with a cre-dependent GCaMP8-coding virus in TH-cre rats, for simultaneous optogenetic stimulation and photometry recordings in the B) VTA or SNC. C) Z-score average trace of DA neuron fluorescence time locked to 5-Hz stimulation ($n=10$). Robust phasic DA neuron activation was seen, as measured by signal D) peak and E) area under the curve (AUC) measures. F) DA neuron activity diminished quickly following laser termination. G) Z-scored trace of DA neuron fluorescence time locked to 20-Hz stimulation ($n=9$). Robust sustained DA neuron activation, as measured by signal H) peak and I) AUC measures. J) This signal was slower to diminish following laser termination. K) VTA ($n=4$) and L) SNC ($n=6$) DA neuron activity plotted separately show distinct phasic versus sustained activation patterns at 5 Hz, which differed in M) peak signal, but not N) AUC. O) VTA ($n=4$) and P) SNC ($n=5$) DA neuron activity plotted separately show similar sustained activation patterns at 20 Hz, which did not differ in Q) peak signal or R) AUC. ** $p<.01$ (unpaired t test), * $p<.05$. *** $p<.001$ (one sample t test vs 0), ## $p<.01$ (vs 0), # $p<.05$ (vs 0). Error bars depict SEM.

a brief phasic burst, followed by a small, sustained response. In the SNc, there was no phasic burst, but a steady sustained signal. Comparing the regions directly, the VTA and SNc responses differed in signal peak (Fig 2M; unpaired t test $t(8)=4.03$, $p=.0038$), but not overall AUC (Fig 2N; t test $t(8)=1.172$, $p=.275$) during the stimulation window. At 20 Hz, signals in the VTA and SNc were more similar (Fig 2O,P), both showing sustained increases during the simulation window (Fig 2Q,R; t test for peak $t(7)=1.015$, $p=.344$; t test for AUC $t(7)=.109$, $p=.916$). Together these data show that SC terminals acutely activate dopamine neurons in the VTA and SNc in vivo.

Superior colliculus projections excite VTA GABA neurons *in vivo*

SC terminals have also been shown to also make contact with GABAergic neurons (Comoli et al., 2003; Solié et al., 2022; Z. Zhou et al., 2019), which make up approximately 30% of neurons in the VTA (Nair-Roberts et al., 2008). To determine how SC input affects the activity of these neurons *in vivo*, we combined fiber photometry recordings of GABA neurons with optogenetic activation of SC terminals in the VTA. To target GABA neurons, we used a promoter-based viral strategy (Scott et al., 2023; Wakabayashi et al., 2019). One virus delivered cre-recombinase with transfection driven by the GAD1 promoter, while a second, cre-dependent virus delivered GCaMP8. Through this method we recorded the impact of SC terminal stimulation on GABA neurons in the VTA (Fig 3A,B). GABAergic neurons in the VTA showed a primarily phasic increase in activity (Fig 3C) in response to 5 Hz SC terminal excitation (Fig 3D,E; one sample t

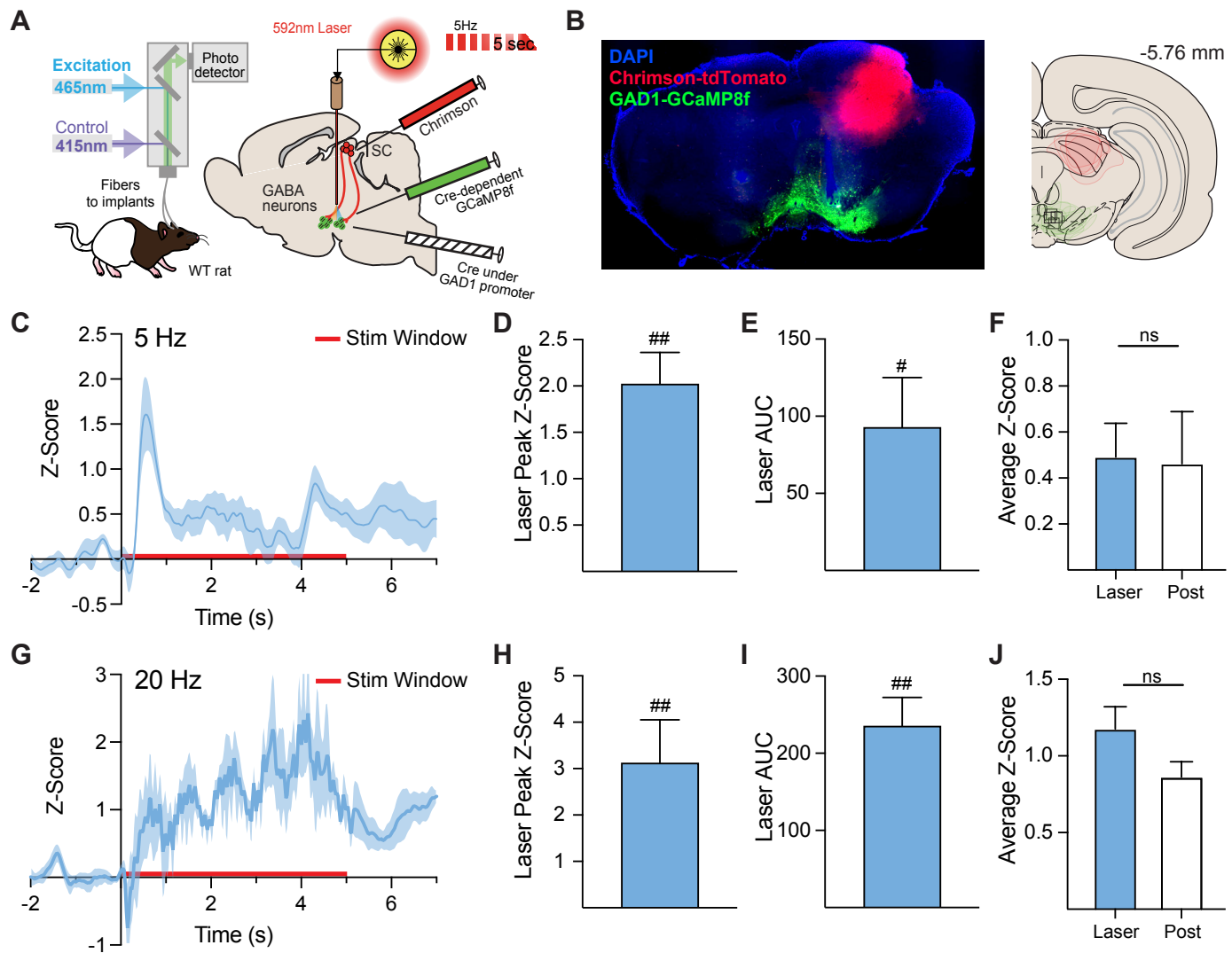


Fig 3. Superior colliculus projections activate GABA neurons in the VTA *in vivo*. Approach to target SC terminals with the red-shifted excitatory opsin ChrimsonR and GABA/GAD1+ neurons with a cre-dependent GCaMP8-coding virus in wild type rats, for simultaneous optogenetic stimulation and photometry recordings in the VTA. C) Z-score averaged trace of GABA neuron fluorescence time locked to 5-Hz stimulation ($n=5$). Robust phasic GABA neuron activation was seen, as measured by signal D) peak and E) AUC measures. F) This signal was slow to return to baseline following laser termination. G) Z-scored trace of DA neuron fluorescence time locked to 20-Hz stimulation ($n=4$). Robust sustained GABA neuron activation was seen, as measured by signal H) peak and I) AUC measures. J) This activity slowly diminished following laser termination. ## $p<.01$ (one sample t test vs 0), # $p<.05$ (vs 0). Error bars depict SEM.

test peak $t(4)=5.98$, $p=.0039$; AUC $t(4)=2.88$, $p=.045$). Stimulation of SC terminals at 20 Hz (Fig 3G) evoked a different pattern, where GABA neuron activity rose more slowly across the stimulation window (Fig 3H,I; t test peak $t(3)=3.36$, $p=.0438$; AUC $t(3)=6.35$, $p=.0079$). At both stimulation frequencies, GABA neuron activity did not immediately return to baseline in the 2 sec following laser termination (Figure 3F,J; paired t test 5Hz t(4)=.209, $p=.845$; 20Hz t(3)=1.467, $p=.239$).

Taking our results (Fig 2 and 3) together, we show that SC neurons projecting to the ventral midbrain excite both dopamine and GABA neurons in the VTA/SNc, with frequency-dependent patterns.

Superior colliculus projections to VTA/SNc do not drive Pavlovian cue learning

Previous studies (Engel et al., 2024; Saunders et al., 2018) have shown that stimulation of dopamine neurons in the SNc and VTA is sufficient to create conditioned responses to an associated, previously neutral cue. We hypothesized that SC projections to dopamine neurons contain sensory information about salient cues, and that these projections may therefore drive Pavlovian conditioned responses. To test this, we employed an

optogenetic Pavlovian conditioning procedure. We expressed ChR2 in deep layer SC neurons and implanted a stimulating optic fiber over the ipsilateral VTA, SNc, or a control region elsewhere in the midbrain (Fig 4A,B). Rats were given 12 sessions wherein presentations of a neutral visual stimulus (cue light, 7 sec) were paired with brief optogenetic excitation of SC terminals (473nm laser, 5 sec, 20Hz). As with our previous studies using this approach (Saunders et al., 2018), no behavioral responses were required to obtain either cue or laser presentations, and no external rewards were given, in order to assess the inherent conditioning power of the circuit. Video recordings of conditioning sessions were first analyzed via hand scoring, with experimenters blind to the animal's implant target. We focused on cue orientation/approach (Fig 4D), a common cue-evoked behavior seen for direct dopamine neuron stimulation, and in response to naturally conditioned stimuli.

Contrary to our prediction, SC terminal stimulation did not drive reliable cue-conditioned behavior. Across training, approach behavior in response to the cue alone remained at a low level for SC-VTA and SC-SNc stimulation groups, similar to the level seen for a control group where laser delivery was targeted outside of the ventral midbrain (Fig 4E; no effect of stim group,

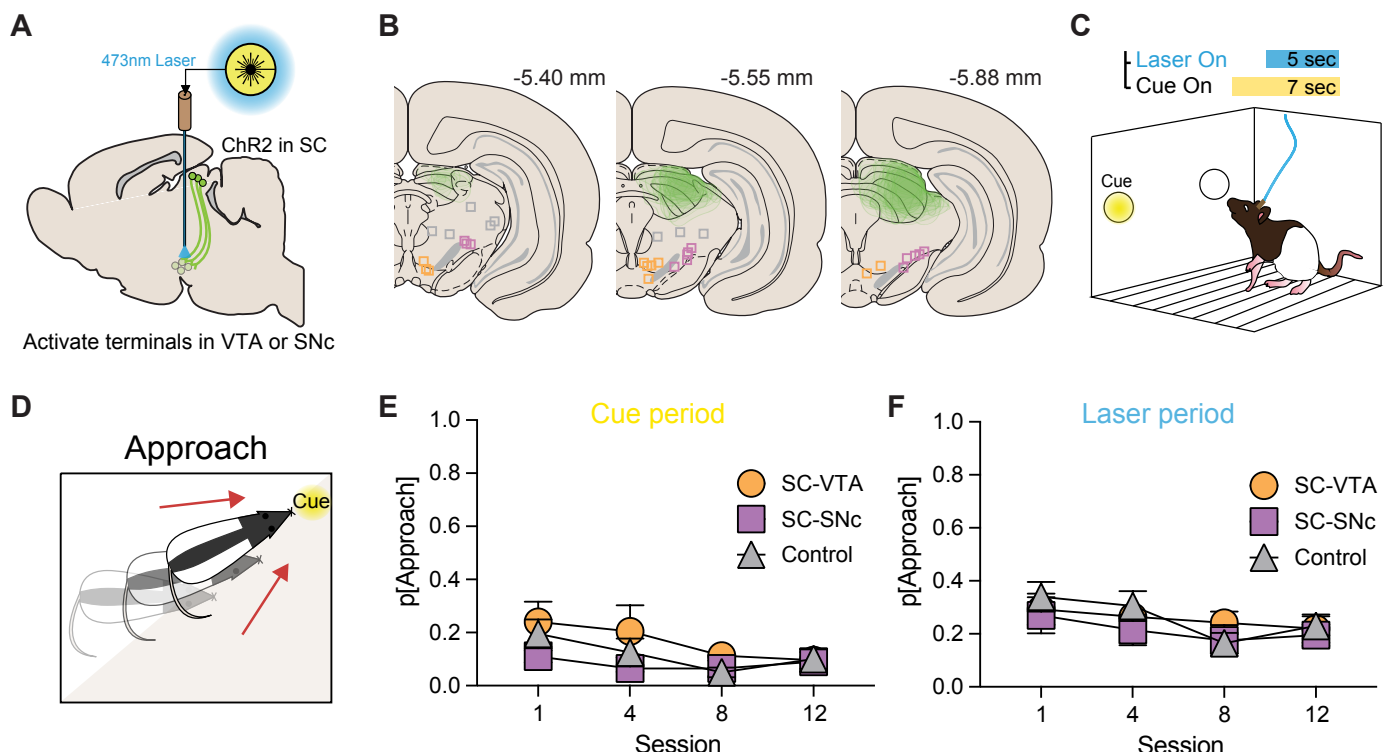


Fig 4. Activation of SC projections to the VTA/SNc does not drive Pavlovian cue conditioning. A) Approach for targeting of SC terminals in the ventral midbrain. ChR2-YFP expressed in deep layer SC neurons, and B) an optic fiber was implanted over the ipsilateral VTA (SC-VTA, $n=6$), SNc (SC-SNc, $n=8$), or a control region (Control, $n=8$). C) Optogenetic Pavlovian conditioning paradigm, where a neutral cue was paired with optogenetic activation of SC terminals. D) Instances of cue approach behavior were measured via inspection of video recordings during conditioning. E) During the cue-only period, corresponding to the first 2-sec of cue presentations, minimal approach behavior occurred across all groups. F) During the laser period, corresponding to the final 5 sec of the cue when laser was also delivered, approach was similarly low for all groups. Error bars depict SEM.

$F(2,19)=2.01$, $p=.16$). The approach behavior that did occur to the cue diminished across training (main effect of session, $F(2.31,43.28)=3.796$, $p=.023$). Focusing on the period of laser stimulation, we again did not see emergence of cue approach for either SC-VTA or SC-SNC groups (Fig 4F; no effect of group, $F(2,19)=.516$, $p=.605$). Thus, in stark contrast to direct dopamine neuron activation (Engel et al., 2024; Saunders et al., 2018), activation of SC neurons projecting to dopamine-rich brain regions, while evoking dopamine neuron

activity, does not imbue neutral stimuli with conditioned value to drive learning.

Superior colliculus projections to VTA/SNC evoke head and body turning

Despite not clearly driving cue learning, examination of rat behavior during the optogenetic conditioning paradigm showed that SC terminal activation produced a consistent motor output, in the form of a head/

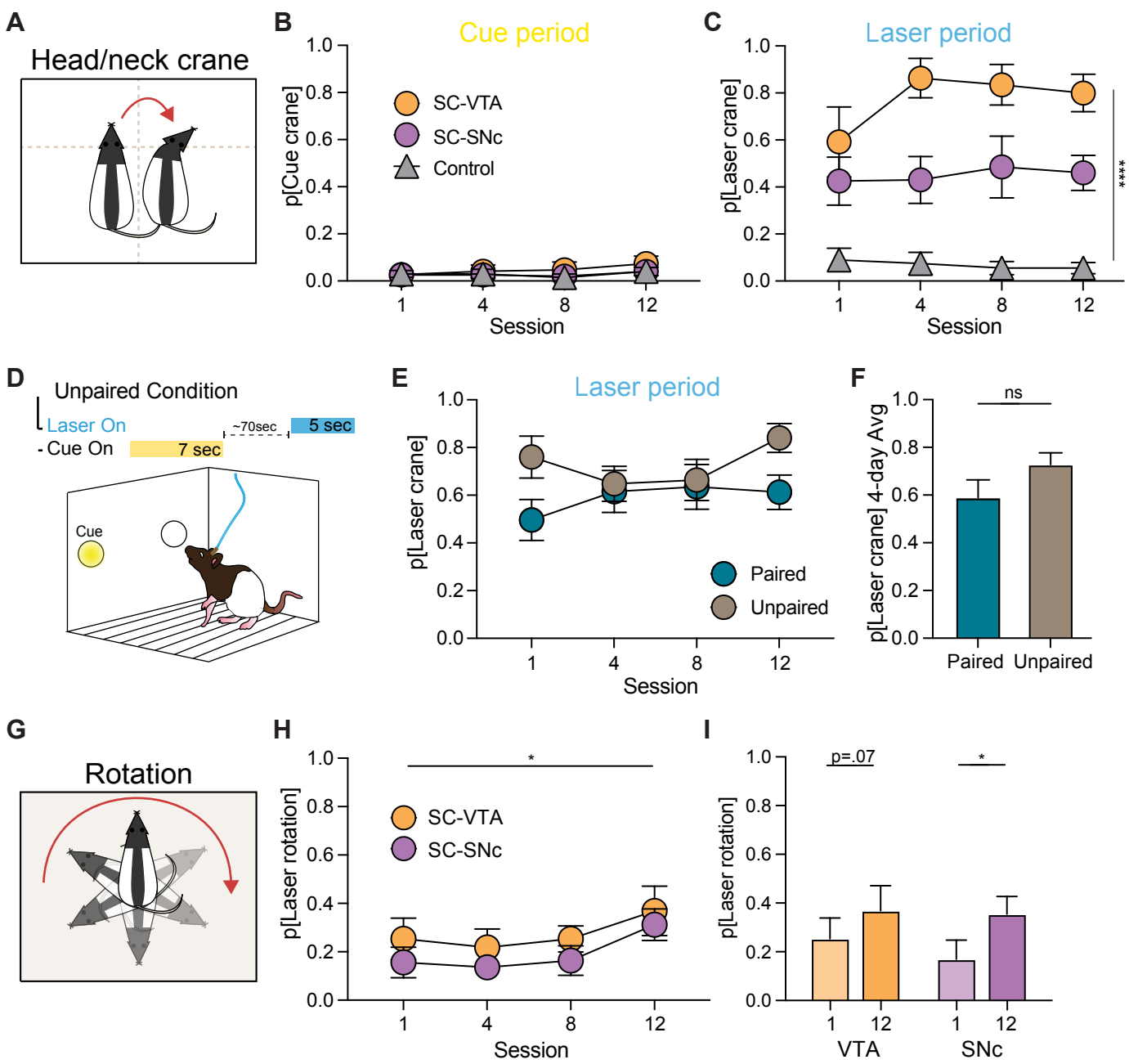


Fig 5. SC terminal stimulation in the VTA and SNC evokes head/neck turning independent of cue conditioning. A) Schematic illustrating craning behavior, which was defined as a head deflection of at least 90 degrees contralateral to the stimulation hemisphere. B) Craning behavior did not occur during the cue-only period (before laser onset). C) During the laser period, craning was robust in the SC-VTA ($n=6$) and SC-SNC ($n=8$) groups relative to controls ($n=8$). D) Unpaired optogenetic conditioning procedure, where cue and laser presentations were separated by a variable interval, for a separate cohort of rats ($n = 5$). E) Unpaired rats exhibited a similar probability of craning as paired subjects across training, and F) when data was collapsed across all analysis sessions. G) In addition to head craning, full body rotation contralateral to the stimulation hemisphere was quantified. (H,I) Rotations during the laser period occurred on a subset of trials, increasing in probability across conditioning sessions for SC-VTA and SC-SNC rats. *** $p<.0001$, * $p<.05$. Error bars depict SEM.

upper body turning. This behavior, which we called a “craning” response, was always directed contralateral to the stimulation hemisphere. For analysis, we operationalized a crane occurring if the rat’s head turned at least 90 degrees, based on a quadrant axis overlaid on the video frame (Fig 5A). Critically, craning behavior did not reliably emerge during the cue-only period (Fig 5B; no effect of stim group, $F(2,19)=.698$, $p=.51$). Instead, we saw reliable heading turning/craning only during the period of laser stimulation. This turning occurred strongly in the SC-VTA and SC-SNc subjects, relative to controls (Fig 5C; main effect of stim location, $F(2,19)=24.05$, $p<.0001$), which showed no consistent behavioral response of any kind. While SC-SNc rats exhibited substantial craning, the probability of craning was even higher in SC-VTA rats, an effect that was clearest by the end of the conditioning paradigm (post hoc comparison VTA vs SNc session 12, $p=.0236$). Although we saw a qualitative increase in the probability of craning in the VTA group across conditioning (Fig 5C, there was no overall change in craning likelihood among groups (no main effect of session, $F(2.45,46.6)=1.66$, $p=.196$).

In our cue-laser paired rats, we saw that turning only clearly occurred during the laser portion of the cue presentation, and not to the cue alone. To examine the effect of the cue presentation on craning, we ran a separate cohort of rats ($n=5$, 3 SC-VTA, 2 SC-SNc) through an unpaired version of the optogenetic conditioning paradigm. In this version, the same number of cue and laser presentations were given across 12 sessions, but each cue and laser event were separated in time and never overlapped (Fig D). These unpaired rats also showed robust craning behavior to laser but not cue presentations. Across conditioning, there was no significant difference in the probability of craning for paired versus unpaired rats during laser stimulation (Fig 5E, no effect of condition, $F(1,17)=1.14$, $p=.301$). Averaged across sessions, unpaired craning was nominally higher than paired, but not significantly different (Fig 5F, unpaired t test, $t(17)=1.07$, $p=.301$). Thus, craning behavior was evoked by SC terminal stimulation, and was not a byproduct of cue-evoked learning.

Craning responses mostly reflected an upper body turn, but in some cases this behavior became a full body rotation, which we also quantified (Fig 5G). As with other behaviors, rotations occurred specifically during laser periods. Across all rats in the SC-VTA and SC-SNc groups, while rotations only occurred on a subset of trials, rotation probability increased across optogenetic conditioning (Fig 5H; main effect of session,

$F(2.05,34.8)=3.96$, $p=.027$), suggesting an overall potentiation in the effect of SC terminal stimulation on turning behavior. Within the SC-VTA group, there was a trend for an increase in rotations from the first to last session (Fig 5I, paired t test, $t(8)=2.01$, $p=.079$), and a significant increase in the SC-SNc group ($t(7)=3.135$, $p=.0165$).

Above, we showed that SC neurons activate dopamine neurons *in vivo*. Increased dopamine activity is often associated with generalized locomotion (Howe & Dombeck, 2016), and repeated dopaminergic activation via pharmacologic (Magos, 1969), optogenetic (Kravitz et al., 2010; Lobo et al., 2010; Saunders et al., 2018), or chemogenetic (Ferguson et al., 2011) manipulation can sensitize locomotion. Therefore, we next examined locomotion more generally, irrespective of cue and laser presentations. To quantify the movement, we used the markerless pose estimation tool, DeepLabCut (Mathis et al., 2018) to identify rat body parts within the chamber. Using this positional data, we calculated the average speed of rats for each conditioning session (session length ~45 min). This analysis revealed that SC terminal stimulation did not produce a general state of hyperactivity. Average movement speed was similar for SC-VTA, SC-SNc, and control rats (No effect of stim location, $F(2,15)=.349$, $p=.717$; avg speed: VTA 6.6 cm/s, SNc 6.26 cm/s, control 5.56 cm/s). Further, repeated stimulation did not produce locomotor sensitization, as average speed did not change across conditioning sessions ($F(2.16,31.7)=1.30$, $p=.287$).

SC projections transiently shape postural reorientation

In Figure 5, we quantified the probability of craning based on an operational cutoff of >90 degrees turned. Across animals, and trial to trial, the extent of turning was variable, and turns were often below our cutoff threshold. To assess this in more detail, we used pose data from our DLC model to determine the degree of reorientation during cue and laser periods (Fig 6). A vector running from the middle of the back to the front of the animal was calculated. The vector’s relative position was compared frame to frame, and the cumulative angle of turning was quantified (Fig 6B,C). This approach revealed that upper body turning was tightly coupled to the laser delivery window in both SC-VTA (Fig 6D) and SC-SNc (Fig 6E) rats, with no turning occurring for anatomical control subjects (Fig 6F).

Overall, the pattern and intensity of turning was similar for SC-VTA and SC-SNc rats, and so we collapsed these groups for remaining analyses. We first compared

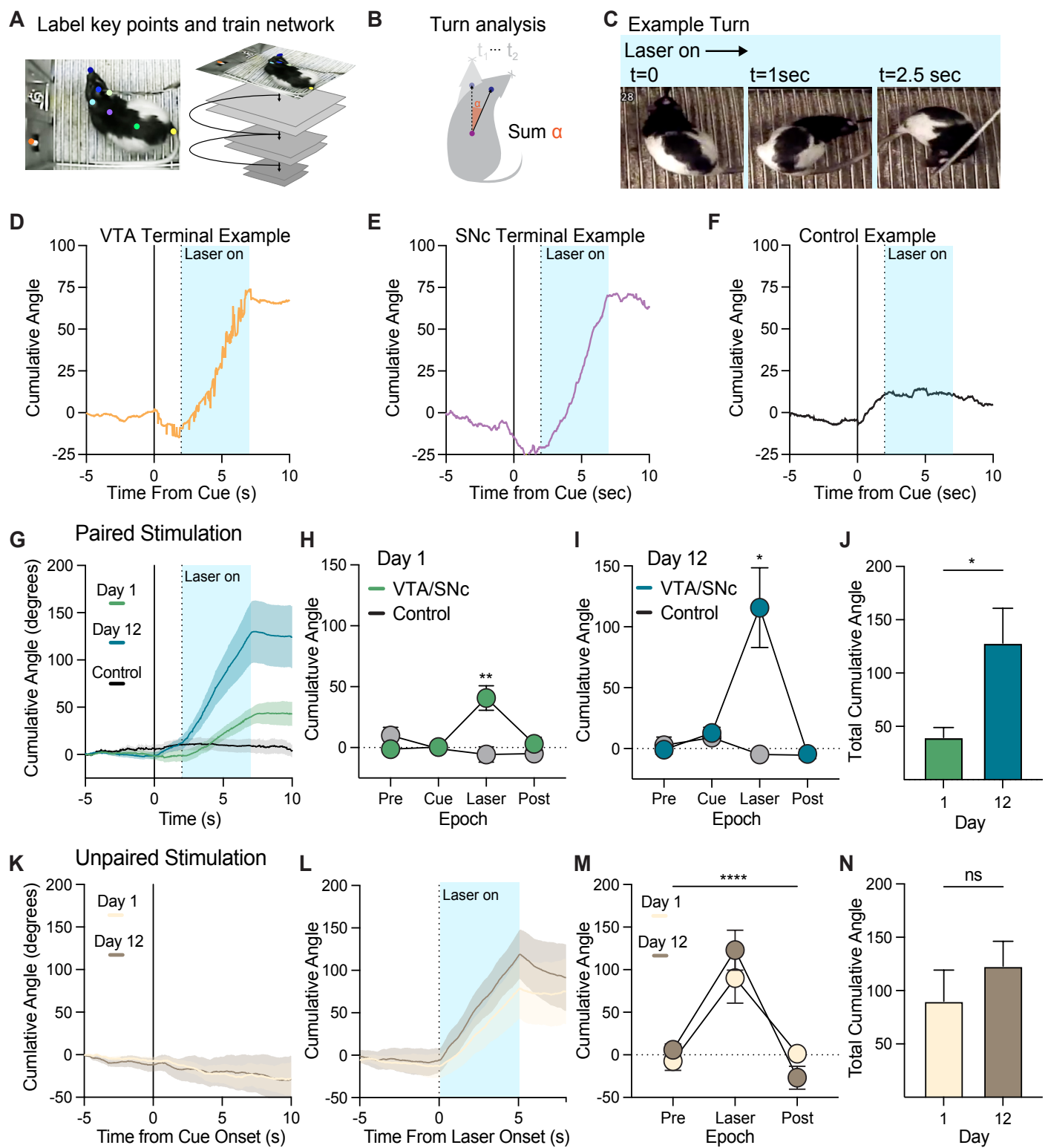


Fig 6. SC projections to VTA/SNC transiently shape head turning. A) Rats' body parts and static elements of the chamber were labeled in video frames from behavior sessions to train a neural network and acquire pose data using the DeepLapCut pipeline. B) A directionality vector was interpolated and tracked across video frames for calculation of turning angle. C) Example turn, showing a rat at three sequential timepoints during a laser stimulation event. Turning examples for D) SC-VTA, E) SC-SNC, and F) control subjects. The blue shaded zone corresponds to the laser stimulation window. A positive slope corresponds to an increase in the cumulative angle of deflection of the head vector contralateral to the hemisphere of laser stimulation. G) Averaged turning traces for paired SC-VTA/SNC rats ($n=12$) on the first and last day of conditioning versus controls. On the H) first and I) last sessions, turning occurred only during the laser period in VTA/SNC rats, and not in controls. J) Laser-evoked turning intensity increased for paired rats from the first to last day of conditioning. K) Average cumulative angle traces for unpaired VTA/SNC rats ($n=5$) show no turning during unpaired cue presentations, but L) robust turning during the laser windows. M) As with paired rats, turning was specific to the laser epoch. N) Unpaired rat turning increased qualitatively, but was not significantly higher on the last day of conditioning. **** $p<.01$, * $p<.05$. Error bars depict SEM.

cumulative turning in the cue-paired rats, plotting angle deflection from cue onset and during the laser period for the first and last conditioning sessions (Fig 6G). The laser-evoked nature of turning was evident in this group data, where a consistent increase in the slope of traces indicates a cumulative increase in the angle of head/neck deflection, specifically during the laser window. Splitting the cumulative angle into epochs showed that significant turning only occurred during the laser window, and not in response to the cue alone, or following termination of laser stimulation, for both the first (Fig 6H; epoch by group interaction, $F(3,45)=7.48$, $p=.0004$) and last (Fig 6I; $F(3,48)=6.02$, $p=.0014$) session of conditioning, relative to controls. Further, we found that for the paired rats, the intensity of turning significantly increased across conditioning (Fig 6J; paired t test, $t(10)=2.76$, $p=.02$), consistent with the increase in rotations shown in Fig 5.

We separately analyzed turning in the unpaired rats. For these animals, no consistent turning occurred in response to cue presentations (Fig 6K). Laser delivery evoked consistent turning, which stopped upon laser termination, similar to the paired rats (Fig 6L,M; main

effect of epoch, $F(1.41,11.27)=28.57$, $p<.0001$). While turning intensity was nominally higher on the last day of conditioning for unpaired rats, this difference was not statistically different (Fig 6N; paired t test, $t(4)=1.37$, $p=.243$). However, when laser-evoked turning for paired and unpaired rats was averaged together, we found a strong significant increase in turning intensity from the first to last session (paired t test, $t(15)=2.95$, $p=.0098$). Collectively, these data indicate that activation of SC terminals in the VTA and SNC promotes a specific, focal behavioral pattern that includes reorientation of the head and neck.

Superior colliculus projections to VTA/SNC do not drive reinforcement or valence assignment

Previous studies show that direct activation of VTA/SNC dopamine neurons supports robust reinforcement (Engel et al., 2024; Fraser et al., 2023; Ilango et al., 2014; Saunders et al., 2018; Tsai et al., 2009), inducing vigorous response patterns to obtain stimulation. Given our finding that SC neurons projecting to the VTA/SNC activate dopamine neurons, we next asked if stimulating these VTA/SNC inputs supports reinforcement. A subset

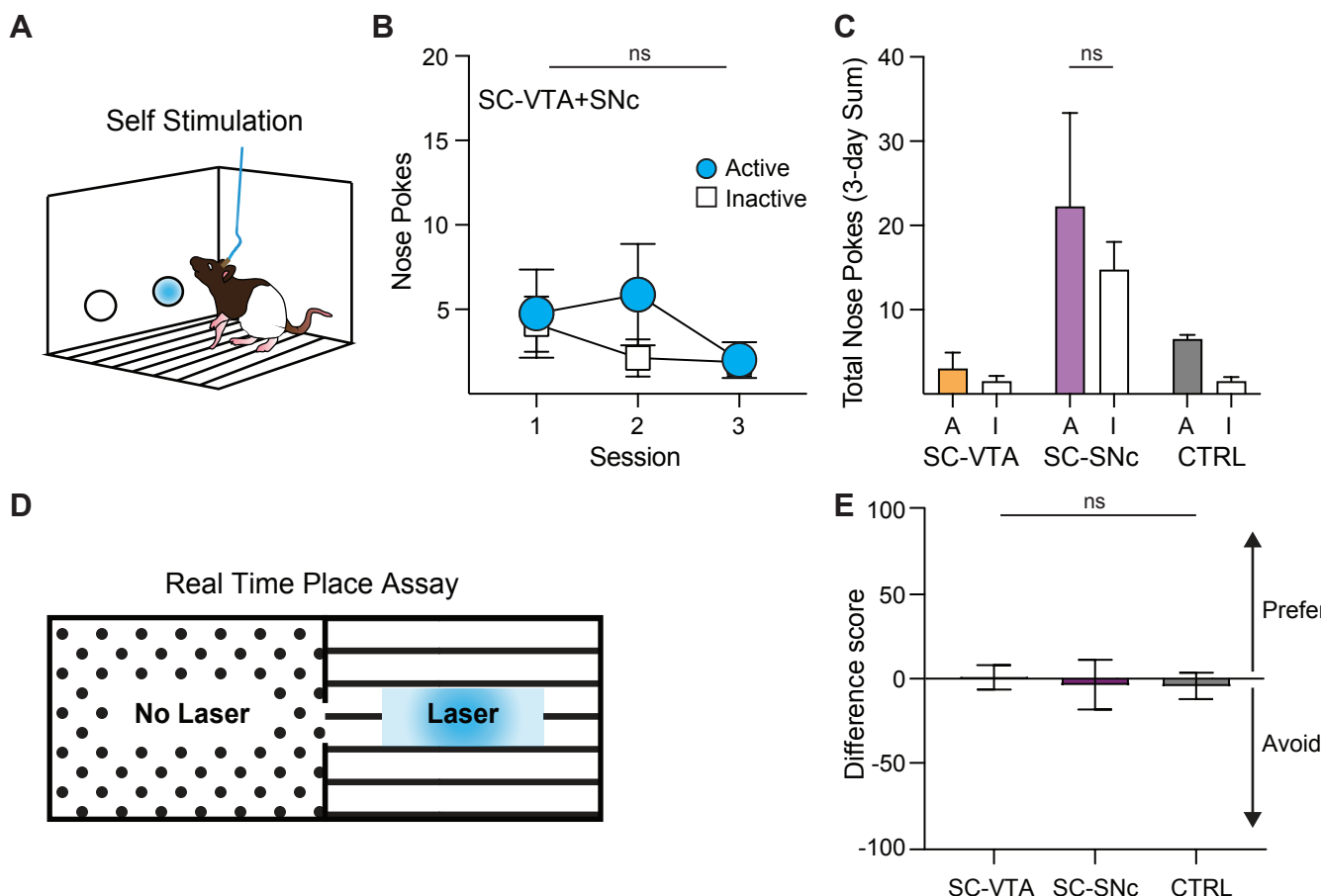


Fig 7. SC terminal stimulation does not support reinforcement or signal valence. A) Intracranial self stimulation (ICSS) set up. B) Nose behavior was low overall ($n=8$). C) Plotted separately, SC-VTA ($n=4$), SC-SNC ($n=4$), and control ($n=2$) groups exhibited low responding, failing to discriminate between active and inactive nose pokes. D) Real time place assay paradigm. E) No preference or avoidance was observed for any group. Error bars depict SEM.

of rats (SC-VTA = 4, SC-SNc = 4, Control = 2) were trained in an intracranial self stimulation (ICSS) task where active nose pokes resulted in delivery of a brief (1-sec) laser stimulation across three sessions (Fig 7A). Overall, rats failed to reliably engage in self-stimulation behavior (Fig 7B; no effect of nose poke, $F(1,14)=.417$, $p = 0.5309$). When examined separately, we found that SC-SNc rats self-stimulated nominally more than either SC-VTA or control subjects (Fig 7C; effect of implant location, $F(2,14)=5.02$, $p = 0.023$), but this reflected an increase in both active and inactive responses, and behavior was very low overall (~ 10 nose pokes/ session).

Finally, we investigated if stimulation of SC terminals in the VTA/SNc drives an overall positive or negative valence, using an optogenetic real time place assay. Rats could move freely between two distinct chambers while tethered to a laser (Fig 7D). When >50% of the body crossed into the laser-paired chamber, SC terminals were optogenetically activated. Laser stimulation ceased when they crossed back into the neutral chamber. A difference score was calculated for each rat, based on the amount of time they spent in the stimulation chamber compared to the control chamber. A value of 100 would indicate the animal spent 100% of their time in the stimulation paired chamber, whereas a value of -100 would indicate the animal spent 100% of their time in the neutral chamber. There was no effect of stimulation location on difference score (Fig 7E; $F(2,10)=.007$, $p = 0.9301$). There was no side preference for any group, and all rats spent a relatively equal amount of time in both chambers, suggesting that stimulation was not strongly rewarding or aversive.

DISCUSSION

In these studies, we investigated the anatomical organization and functional role of superior colliculus neurons projecting to the dopaminergic midbrain. Our primary findings are: 1) Deep layer SC neurons anatomically interface with dopamine neurons in the VTA and SNc. 2) SC projections excite dopamine neurons in both the VTA and SNc, and GABA neurons in the VTA *in vivo*. Despite this, optogenetic excitation of SC projections to the VTA and SNc was not sufficient to drive Pavlovian learning about associated cues, nor did it promote reinforcement or aversion. Instead, we found that stimulation of SC inputs to the VTA/SNc spurred head turning and body reorientation, and this motor effect potentiated with time. These results offer insights into a number of ongoing questions related to learning and attentional mechanisms impinging on midbrain circuitry.

SC projections exert nuanced control over ventral midbrain neurons

We find that deep layer SC neurons project to and excite dopamine neurons in the VTA and SNc. This is consistent with previous studies (Comoli et al., 2003; Dommett et al., 2005; May et al., 2009; McHaffie et al., 2006; Redgrave, Coizet, Comoli, McHaffie, et al., 2010), and we extend this work to show this process happens *in vivo* in behaving rats. We find some subtle differences in the pattern and timing of evoked dopamine signals depending on the frequency of SC input. This suggests SC can exert nuanced control over the dopamine system, potentially, along with other inputs, modulating tonic and phasic-related activity modes in different behavioral contexts (Berke, 2018; Bromberg-Martin et al., 2010b; Grace et al., 2007; Tian et al., 2016; Wise & Robble, 2020). Previous electron microscopy results show that SC projections to the ventral midbrain synapse on non TH-containing neurons (Comoli et al., 2003; Redgrave, Coizet, Comoli, McHaffie, et al., 2010), including the notable population of GABA neurons that reside in the VTA (Nair-Roberts et al., 2008). We find that the SC directly activates VTA GABA neurons, in line with more recent studies using genetic tools (Z. Zhou et al., 2019). The local interplay between GABA and dopamine neurons receiving input from the SC is unclear, but our results suggest that the bulk effect of SC-GABA excitation is not to simultaneously inhibit local dopamine neurons. One possibility is that SC inputs target GABA neurons that primarily project out of the VTA, including to frontal regions like the striatum or cortex (Solié et al., 2022; Taylor et al., 2014; W.-L. Zhou et al., 2022; Z. Zhou et al., 2019). Further, some SC neurons likely also interface with GABA neurons in the pars reticulata portion of the substantia nigra, the specific role of which is unclear. It will be critical to further dissect the regional and microcircuit influences SC neurons have within the ventral midbrain.

The direct activation of dopamine neurons in the SNc/VTA drives strong learning and value assignment (Coizet et al., 2007; Engel et al., 2024; Fraser et al., 2023; Huang et al., 2021; Ilango et al., 2014; Saunders et al., 2018; Tsai et al., 2009). Surprisingly, despite clearly activating dopamine neurons in the VTA and SNc *in vivo*, here we found that optogenetic activation of SC projections to these regions does not drive Pavlovian conditioning, or promote reinforcement. While it is tempting to assume that the negligible effect of SC inputs on learning may be due to the co-activation of GABA neurons in the VTA, SC inputs to the SNc similarly failed to drive Pavlovian conditioned cue valuation and clear reinforcement, despite activating dopamine neurons there. Given that

dopamine neurons in the SNC are not intermingled with local GABA neurons as in the VTA, this suggests that the lack of learning via SC terminal stimulation is not simply due to the co-activation of GABA neurons. A large literature now indicates that SNC and VTA dopamine neurons subserve unique learning and motivational functions (Collins & Saunders, 2020; Cragg et al., 1997; Ikemoto, 2007; Keiflin et al., 2019; Lammel et al., 2008; Tian et al., 2016; Ungless & Grace, 2012; Watabe-Uchida et al., 2012). Here, we find qualitatively similar effects for SC terminal stimulation in the VTA and SNC, in terms of behavior and dopamine activation. One possibility is that SC may activate a subset of VTA/SNC neurons distinct from populations activated in previous studies demonstrating motivation and reward.

While many dopamine neurons are thought to encode reward prediction errors, individual circuit inputs do not transmit all features of reward-prediction errors independently, instead signaling mixed and distributed functions that differentially contribute to learning (Beier et al., 2015; Bromberg-Martin et al., 2010a; Engelhard et al., 2019; Farassat et al., 2019; Lerner et al., 2015; Tian et al., 2016). This suggests that an integrative computation of the complete input activity to a dopamine neuron accompanies learning. Our results add to this notion, to show that a prominent sensorimotor input from the SC is insufficient to drive learning on its own. Collectively, this underscores an important conclusion borne out by our data: activation of dopamine neurons is not part and parcel with learning and reinforcement, and not all circuit inputs that activate dopamine neurons necessarily promote these processes. For “complete” learning to occur, other components of a rewarding outcome (such as gustatory signals for food) may need to be incorporated into VTA/SNC in order to create a learned response. The VTA and SNC are known to receive a variety of sensory and homeostatic afferents (Boughter et al., 2019; Watabe-Uchida et al., 2012), and without the co-activation from these other inputs, it is not possible to create a conditioned cue-response from Pavlovian conditioning. Indeed, it has been suggested that the neural correlates of learning and value are likely distributed between inputs to dopamine centers (Bromberg-Martin et al., 2010b; Tian et al., 2016; Watabe-Uchida et al., 2012). It will be important to further explore what specific role SC inputs to dopamine neurons play within this set of computations.

SC neurons activate dopamine for alerting, not reward prediction

While SC activation of dopamine neurons in the VTA/SNC failed to create conditioned behavior to predictive

cues, we saw the emergence of specific movement patterns: rats crane their heads and necks during SC terminal stimulation. This behavior showcases the control the SC has over head/neck (Cregg et al., 2020), and general contributions to exploration. Reorientation of the head promotes survey of the environment, for successful identification and navigation around potentially rewarding or harmful stimuli. The deep layers of superior colliculus are known for coordinating exploratory behavior, via control of orientation (Isha et al., 2019; Suzuki et al., 2019; Villalobos & Basso, 2020) and attentional shifts (de Araujo et al., 2015; Goldberg & Wurtz, 1972; Hoy et al., 2019; Ignashchenkova et al., 2004; Krauzlis et al., 2013; White & Munoz, 2011; Yoshida et al., 2012). The ability to orient to potentially salient stimuli at rapid latencies is an important step in learning about cued outcomes, and could provide insight into the function of SC-induced dopamine excitation. Notably, we saw evidence of a potentiation of the motor effect of SC terminal stimulation. This suggests that some level of plasticity is engaged when SC inputs to the VTA/SNC are repeatedly activated. Future studies will be important for determining the specific conditions under which this occurs. Individual VTA dopamine neurons are sensitive to head position and movement kinematics (Engelhard et al., 2019; Hughes et al., 2020), and it is tempting to speculate that property could be driven in part by SC inputs. Strengthening the head turning effect to reorient gaze to a particularly salient stimulus more rapidly over time could be one way that SC engages motor patterns (Basso et al., 2021; Hopp & Fuchs, 2004), via integration with dopamine areas, to promote attentional bias across learning.

While dopamine is classically associated with reward-prediction error, our data suggest that rapid dopamine activation in response to visual cues likely does not represent reward prediction error or value-imbuing signal (Amo, 2023; Berke, 2018; Lerner et al., 2021; Schultz, 1998). Instead, our results support the proposal that low-latency dopamine neuron activation acts as an alerting signal (Bromberg-Martin et al., 2010a; Redgrave et al., 1999; Schultz, 2007), conveying that an important stimulus is present and should be further investigated. Such a signal does not reflect the value of the stimulus (positive or negative), but instead, prompts the animal to coordinate motor patterns to explore the stimulus further. These patterns likely include manipulation of head and neck posture, much like the craning we see when stimulating SC-VTA/SNC pathways. The rapid coordination of movements in both investigatory and avoidance contexts is shown to be controlled by SC projections in important recent studies. For example, deep layer SC projections to the VTA/SNC contribute

to fear-induced escape and avoidance (Almada et al., 2018; Sahibzada et al., 1986; Z. Zhou et al., 2019) while also signaling appetitive behaviors such as head orientation to conspecifics (Solié et al., 2022) and motion towards prey (Almada et al., 2018; Huang et al., 2021). When such inherently valuable stimuli are absent from the environment, as in our studies, we find that SC inputs to drive dopamine neuron activity do not artificially instantiate valuation. The ability of this pathway to create motor outputs to both positively and negatively valenced events is also consistent with the lack of either ICSS or place preference observed (Solié et al., 2022).

A full understanding of the functional role of SC inputs to the VTA/SNC will require further experimentation. It will be important, for example, to isolate the contribution of SC neurons that project only to dopamine neurons in the VTA, versus those projecting to VTA GABA neurons, glutamate neurons, and/or other unique ventral midbrain populations (Prévost et al., 2024). Additionally, we show that SC projects to VTA/SNC target neurons that project to motivated behavior centers like striatum and ventral pallidum. Further investigation of this tectum-meso/nigro-frontal network will support a more complete view of the likely multiple channels of influence collicular systems have on adaptive behavior (Chevalier & Deniau, 1984; Cover et al., 2024; Lak et al., 2020; Lee et al., 2020; Lee & Sabatini, 2021; Mana & Chevalier, 2001), and disease (Bellone et al., 2024).

In conclusion, our results highlight a brain circuit that is important for guiding movement to redirect attention, via interaction with classic learning systems. We find that deep layer SC neurons rapidly excite dopamine neurons in both the VTA and SNC, and this activation spurs exploratory movement of space. While this circuit alone does not evoke associative learning, it may be important for priming key learning centers, like dopamine neurons, to important stimuli, for facilitation of association formation.

Funding

This work was supported by NIH grants T32 DA007234 and F31 DA055482 (CLP) and R00 DA042895, R01 MH129370, and R01 MH129320 (BTS).

METHODS

Subjects

Male and female wild type and transgenic TH-cre (Witten et al., 2011) Long-Evans rats (N=48, 22 males, 26 females) were used in these studies. After surgery, rats were dual-housed with littermates and provided *ad libitum* access to food and water on a 0800 to 2000 light/dark cycle (lights on at 0800). All rats weighed >200g at the time of surgery and were between 4-6 months old at the time of experimentation. Experimental procedures were approved by the Institutional Animal Care and Use Committee at the University of Minnesota, Twin Cities and were carried out in accordance with the guidelines on animal care and use of the US National Institutes of Health.

Viral vectors

To visualize superior colliculus (SC) terminals in the VTA and SNC, we used a GFP-expressing virus (AAV5-hsyn-GFP, Addgene). For the visualization of synaptic contact between SC terminals and neurons in the VTA/SNC, a virus coding for membrane bound GFP and mCherry conjugated to the synaptic protein Synaptophysin was used (AAV5-hsyn-mGFP-2A-synaptophysin-mRuby, Addgene). To visualize VTA/SNC neurons receiving direct SC input, we used an anterograde tracing approach exploiting the transsynaptic properties of AAV1 (Zingg et al., 2017). A cre-delivery virus, AAV1-hsyn-cre-WPRE was injected into deep layer SC. Then, a cre-dependent virus expressing mCherry (AAV5-hsyn-DIO-mCherry, Addgene) was injected into the VTA/SNC, allowing for visualization of neurons receiving SC innervation. For combined optogenetic stimulation and photometry experiments, excitation of superior colliculus terminals was achieved via expression of the red-shifted excitatory opsin, ChrimsonR (AAV5-syn-ChrimsonR-tdT; Addgene, Klapoetke et al., 2014), injected into SC. For photometry recordings of dopamine neurons, Cre-dependent expression of the fast and sensitive calcium indicator, GCaMP8f (Zhang et al., 2023), was achieved via injection of AAV5-syn-DIO-jGCaMP8f-WPRE (Addgene) into the VTA and SNC of TH-cre rats. For photometry recordings of GABA neurons, expression of GCaMP8f in GAD+ neurons was achieved through the combination of a cre-delivery virus GAD1-cre (AAV5-GAD1-cre, University of Minnesota Viral Vector and Cloning Core) and a cre-dependent virus expressing GCaMP8f (AAV5-syn-DIO-jGCaMP8f-WPRE, Addgene) injected into the VTA of wild type rats (Scott et al., 2023). For optogenetic conditioning experiments, expression of channelrhodopsin in SC terminals was achieved via injection of AAV5-hsyn-hChR2-EYFP (Addgene) into SC.

Surgical procedures

Viral infusions and optic fiber implants were carried out as previously described (Engel et al., 2024; Steinberg et al., 2014). Rats were anesthetized with 5% isoflurane and placed in a stereotaxic frame. Rats were administered saline, carprofen anesthetic, and cefazolin antibiotic subcutaneously. The top of the skull was exposed and holes were made for viral infusion needles, optic fiber implants, and four skull screws. Following skull exposure, surgery anesthesia was maintained at 1–3%. Viral injections were made using a microsyringe pump at a rate of 0.1 $\mu\text{l}/\text{min}$. Injectors were left in place for 5 min, then raised 100 μm dorsal to the injection site, left in place for another 10 min, then removed slowly. Implants were secured to the skull with dental acrylic applied around skull screws and the base of the ferrule(s) containing the optic fiber. At the end of all surgeries, topical anesthetic and antibiotic ointment was applied to the surgical site, rats were removed to a heating pad and monitored until they were ambulatory. Rats were monitored daily for 1 week following surgery. Optogenetic manipulations commenced 6–8 weeks after surgery.

For photometry recording of dopamine neurons, DIO-GCaMP8f was infused (0.5 μL at each target site for a total of 1 μL per rat) at the following coordinates from Bregma: VTA: posterior -5.4mm, lateral +0.8, ventral -8.1; SNC: posterior -5.4mm, lateral -2.6, ventral -7.3. To record GABA neurons, GAD1-cre and DIO-GCaMP8f were co-infused (0.5 μL each, for a total volume of 1 μL per rat) into the VTA (posterior -5.4, lateral +0.8, ventral -8.1). For optogenetic targeting of SC projections to the VTA and SNC, ChrimsonR (0.5 - 1 μL per side, for a total volume of 1-2 μL per rat) was also injected into deep layer SC at posterior -6.3, lateral +2.0, ventral -4.8. For simultaneous optogenetic activation of SC terminals and photometry recording of dopamine or GABA neurons, low-auto-fluorescence optic fiber implants (400- μm glass diameter, Doric) were inserted just above viral injection sites at the following coordinates. VTA: posterior -5.4, lateral +1.0, ventral -7.8. SNC: posterior -5.4, lateral -2.6, ventral -7.2.

For optogenetic Pavlovian conditioning, ICSS, and RTPP experiments, hChR2 was delivered unilaterally (1 μL total volume per rat) to deep layer SC (posterior -6.3, lateral +2.0, ventral -4.8). Optic fibers (300-nm diameter, custom made) were placed over ipsilateral VTA (posterior -5.4, lateral +0.8, ventral -7.5) or ipsilateral SNC (posterior -5.4, lateral -2.4, ventral -7.2). Subjects with targeting that ended up outside of the VTA/SNC were analyzed separately as anatomical comparisons.

Optogenetic Stimulation

ChrimsonR studies used 590-nm lasers and ChR2 studies used 473-nm lasers (Dragon Lasers), adjusted to produce \sim 2mW/mm 2 light output from the tip of the intracranial fiber during individual 5-ms light pulses used in experiments. Light power was measured before and after every behavioral session to ensure that all equipment was functioning properly. For all optogenetic studies, optic tethers connecting rats to the rotary joint were sheathed in a lightweight armored jacket to prevent cable breakage and block visible light transmission.

Habituation and optogenetic Pavlovian training.

Optogenetic Pavlovian training was based on the behavioral protocol described in previous studies (Engel et al., 2024; Saunders et al., 2018). Briefly, rats were first acclimated to the behavioral chambers (Med Associates), conditioning cue, and optic cable tethering in a ~30-min session. During this session, 25 cue presentations, with no other consequences, were delivered on a 90-s average variable time (VT) schedule. In each of 12 subsequent conditioning sessions, rats in paired groups ($n=22$) were presented with 25 cue (light, 7s) – laser stimulation (100 5-ms pulses at 20 Hz; laser train initiated 2 s after cue onset) pairings delivered on a 200-s VT schedule. Rats in the unpaired group ($n=5$) also received 25 cue presentations and 25 laser trains per session, but an average 70-s VT schedule separated these events in time. These cues were never associated with another external stimulus (for example, food or water). The duration of laser stimulation was chosen to mimic the multi-second dopamine neuron activation observed *in vivo* when these subjects consumed natural reward, such as sucrose (Saunders et al., 2018). In all groups, cue and laser delivery were never contingent on an animal's behavior and all rats received the same number of cue and laser events.

Intracranial self stimulation (3, 1-h sessions). A subset of rats ($n = 12$) were tethered to patch cables in the Med Associates boxes for self stimulation assessment. During these sessions, nose poke ports were positioned on the wall opposite of the cue lights and levers from previous phases. During 3 1-h sessions, pokes in the active port resulted in a 1-s laser train (20 Hz, 20 5-ms pulses, fixed-ratio 1 schedule with a 1-s timeout during each train), but no other external cue events, to assess the reinforcing value of stimulation itself. Inactive nose pokes were recorded, but had no consequences.

Real time place assay (2, 30 min sessions). A subset of rats (unique from ICSS, $n = 12$) were tethered to patch cables and then habituated to a large open top

arena (total arena size: 24"x16"x16") split into two equally sized sections (12"x16"x16"). Each section had a uniquely textured floor and side panels (stripes or dots) distinguishing the two sections. Rats could move freely between both sections. Rats were placed in the center of the arena, and total time spent in each section was recorded throughout 30 min. Time was recorded as being in one chamber if > half of the rat's body was located in the chamber. Times were totaled for each animal, and laser delivery was assigned to each rat's less preferred chamber. The following day, rats were once again placed in the center of the chamber, and an experimenter observed the animals through a camera mounted above the arena for 30 min. When an animal crossed to the laser-paired side, stimulation was delivered (5mW, 5-ms pulses at 20 Hz) for the duration the rat was in said laser-paired chamber. When the rat crossed back to the non-laser side, stimulation ceased. To total the amount of time spent in each chamber, an experimenter blinded to the conditions watched the recorded videos and totaled time spent in each section. A difference score was calculated by subtracting the amount of time spent in the non-laser chamber from the amount of time spent in the laser-paired chamber.

Video Scoring

Behavior during Pavlovian conditioning sessions was video recorded using cameras (VANXSE CCTV 960H 1000TVL HD Mini Spy Security Camera 2.8-12mm Varifocal Lens Indoor Surveillance Camera) positioned a standardized distance above each chamber. Videos from sessions 1, 4, 8, and 12 were scored offline by observers who were blind to the identity and anatomical target group of the rats. Each cue (7 s, 25 per session) and laser (5 s, 25 per session) event was scored for the occurrence and onset latency of the following behaviors. Locomotion was defined as the rat moving all four feet in a forward direction (that is, not simply lifting feet in place). Cue approach was defined as the rat's nose coming within 1 in of the cue light (trials in which the rat's nose was in front of the light when it was presented were not counted in the approach measure). Approach often involved the rat moving from another area of the chamber to come in physical contact with the cue light while it was illuminated. Rearing was defined as the rat lifting its head and front feet off the chamber floor, either onto the side of the chamber, or into the air. Rotation was defined as the rat making a complete 360-degree turn in one direction. Head turning/craning was defined as the rat's head turning at least 90-degrees in one direction, based on visual assessment of the rat's head/neck position relative to a grid overlaid onto the video frame.

DeepLabCut-based behavioral analysis

Markerless tracking of rat body parts and position was conducted using the DeepLabCut (DLC) Toolbox (Mathis et al., 2018) and analysis of movement features based on these tracked coordinates was conducted in Matlab R2021b (Mathworks). DLC analysis was conducted on a Dell G7-7590 laptop running Windows 10 with an Intel Core i7-9750H CPU, 2.60Ghz, 16 GB RAM, and an NVIDIA GeForce RTX 2080 Max-Q 8GB GPU. DeepLabCut 2.1.10 was installed in an Anaconda environment with Python 3.7.7 and Tensorflow 1.13.1. Videos (944 x 480 resolution) were recorded with a sampling frequency of 30 frames per second using a Tiger Security Super HD 1080P 16-Channel DVR system.

DeepLabCut model

For animal tracking we refined a network generated in our previous studies (Engel et al., 2024). Body parts and environmental features were labeled in 2090 frames from 35 videos (from 32 different animals) and refined the network by adjusting 807 outlier frames. 95% of these labeled frames were used for training. We used a ResNet-50 based neural network model for 1,030,000 training iterations. After final refinement and using a p-cutoff of 0.85, training error was 2.99 pixels and test error was 3.68 pixels. The body parts labeled included the nose, eyes, ears, fiber optic implant, midpoint of the shoulders, tail base, and an additional three points along the spine. Features of the environment were also labeled, including the 4 corners of the apparatus floor, two nose ports, two cue lights, two magazine ports, and 3 LED indicator lights when active.

To time-lock behavior to ongoing experimental variables (such as the onset of lights and laser stimulation) a separate network was trained to identify the onset of the cue light and the laser indicator light using 480 frames from 12 videos (10 different animals) and a 95% training dataset. We used a ResNet-50 based neural network model for 1,000,000 training iterations and the training error was 1.39 pixels and the test error was 1.56 pixels after final refinement of outlier frames.

DLC coordinates and confidence values for each body part and environment feature for every frame were imported to Matlab and filtered to exclude body parts/features from any frame where the confidence was < 0.7. To convert pixel distances to the real chamber dimensions, for each video, a pixel to cm conversion rate was determined. The distance (in pixels) between each edge of the environment floor and the diagonal measurements from corner to corner was measured, and these values were divided by the actual distance

in cm. The mean of these values was then used as the conversion factor. Movement speed was calculated from the implant coordinates frame by frame using the formula: [distance moved (pix per cm) * framerate] to give movement speed in cm/s. For detailed analysis of postural turning, cumulative angle was calculated by adding the change in angle (degrees) between the vector between the shoulder point and the mid back point on the current frame and this same vector in the previous frame using the formula: angle= atan2(norm(cross(a,b)), dot(a,b)). Resulting angle values were normalized for the implant hemisphere so that increases in cumulative angle reflected the movement direction (contralateral to the implant).

Fiber photometry

Dopamine neurons in the VTA and SNC of TH-cre rats ($n=10$) were transfected with a cre-dependent GCaMP8f and SC neurons were transfected via the red-shifted opsin ChrimsonR. VTA GABA neurons were targeted with GCaMP8f in a separate cohort of rats ($n = 4$). Implantation of optic fibers in the VTA and SNC allowed for simultaneous optogenetic activation of SC terminals and measurement of activity-dependent fluorescence in the same region (Kim et al., 2016; Saunders et al., 2018).

Photometry was conducted similar to previous studies (Engel et al., 2024; Lerner et al., 2015; Saunders et al., 2018). A fluorescence mini-cube (Doric Lenses) transmitted light streams from a 465-nm LED sinusoidally modulated at 211 Hz, and a 415nm LED modulated at 531 Hz. LED power was set at $\sim 50 \mu\text{W}$. The mini-cube also transmitted light from a 590-nm laser, for optogenetic activation of ChrimsonR through the same low autofluorescence fiber cable (400 nm, 0.48 NA), which was connected to the optic fiber implant on the rat. GCaMP8f fluorescence from neurons below the fiber tip in the brain was transmitted via this same cable back to the mini-cube, where it was passed through a GFP emission filter, amplified, and focused onto a high sensitivity photoreceiver (Newport, Model 2151). Demodulation of the brightness produced by the 465-nm excitation, which stimulates calcium dependent GCaMP8f fluorescence, versus isosbestic 415-nm excitation, which stimulates GCaMP8f in a calcium-independent manner, allowed for correction for bleaching and movement artifacts. A real-time signal processor (RZP, TuckerDavis Technologies) running Synapse software modulated the output of each LED and recorded photometry signals, which were sampled from the photodetector at 6.1 kHz. The signals generated by the two LEDs were demodulated and decimated to 382 Hz for recording to disk. For analysis, both signals

were then downsampled to 40 Hz, low-pass filtered, and a least-squares linear fit was applied to the 415-nm signal, to align it to the 465-nm signal. This fitted 415-nm signal was used to normalize the 465-nm signal, where $\Delta F/F = (465\text{-nm signal} - \text{fitted } 415\text{-nm signal}) / (\text{fitted } 415\text{-nm signal})$. Laser presentation was time stamped in the photometry data file via a signal from the Med-PC behavioral program, and behavior was video recorded as described above. Normalized signals for each stimulation trial were extracted in a window from 5 s preceding to 10 s after laser onset, and Z-scored to the 5 s pre-laser period. Signal peak and area under the curve (AUC) values were calculated from the Z-scored traces by numerical integration via the trapezoidal method using the trapz function (Matlab).

For recording experiments, rats first underwent a day of tether training, wherein they were attached to optic cables and free to explore the chamber. Rats then received 2 counterbalanced stimulation-recording sessions, one with stimulation delivered at 20 Hz, and one with stimulation delivered at 5 Hz. In each of these sessions, 10 unsignaled laser trains ($\sim 2\text{mW } 50 \text{ ms pulses, } 5 \text{ sec train}$) were delivered on a 400-s variable time interval.

Statistics, data collection, and analysis

Rats were randomly assigned to conditioning groups (paired, unpaired) following surgery. Behavioral data from optogenetic conditioning experiments was automatically recorded with Med-PC software (Med Associates) and analyzed using Prism 10.0. Video of conditioning sessions was recorded using a Tiger Security Recording System, and behavior data was analyzed in MATLAB. For manual video scoring, experimenters were blind to the anatomical group identity. Two-way repeated measures ANOVA was used to analyze changes in behavior among the groups across training. Bonferroni-corrected post hoc comparisons and t tests were made to compare groups on individual sessions. No statistical tests were used to predetermine sample sizes, but our sample sizes were similar to previously published studies. Photometry data were collected with TDT Synapse software and analyzed using MATLAB. All comparisons were two tailed. Data in figures are expressed as the mean \pm s.e.m. Statistical significance was set at $p < 0.05$.

Histology

Rats received i.p. injections of Fatal-Plus (2 ml/kg; Patterson Veterinary) to induce a deep anesthesia, and were transcardially perfused with cold phosphate buffered saline (PBS) followed by 4% paraformaldehyde (PFA). Brains were removed and post-fixed in 4% PFA

for ~24 h, then cryoprotected in a 30% sucrose in PBS for 48 h. Fluorescence from viral injections as well as optic fiber damage location was visualized using standard immunohistochemical approaches. Brain sections were cut at 50 µm on a cryostat (Leica Biosystems). For tyrosine hydroxylase (TH) visualization, we completed immunohistochemistry. Sections were washed in PBS and incubated with bovine serum albumin (BSA) and Triton X-100 (each 0.2%) for 20 min. 10% normal donkey serum (NDS) was added for a 30-min incubation, before primary antibody incubation (rabbit anti-TH, 1:500, Fisher Scientific) overnight at 4 °C in PBS with BSA and Triton X-100 (each 0.2%). Sections were then washed and incubated with 2% NDS in PBS for 10 min and secondary antibody was added (1:200 Alexa Fluor 594 donkey anti-rabbit) for 2 h at room temperature. Sections were washed twice in PBS, mounted on microscope slides, and coverslipped with Vectashield containing DAPI counterstain. Fluorescence from synaptophysin-mRuby and mCherry was not amplified. Slides were imaged using a fluorescent microscope (Keyence BZ-X710) with a 4x and 20x air immersion objective. For photometry and optogenetics experiments, rats were included in VTA or SNC groups only if fiber tips were no more than 500 µm dorsal to the target region. Subjects with implants outside of the VTA or SNC were separately analyzed as control/comparison subjects.

REFERENCES

- Almada, R. C., Genewsky, A. J., Heinz, D. E., Kaplick, P. M., Coimbra, N. C., & Wotjak, C. T. (2018). Stimulation of the Nigrothalamic Pathway at the Level of the Superior Colliculus Reduces Threat Recognition and Causes a Shift From Avoidance to Approach Behavior. *Frontiers in Neural Circuits*, 12. <https://doi.org/10.3389/fncir.2018.00036>
- Amo, R. (2023). Prediction error in dopamine neurons during associative learning. *Neuroscience Research*. <https://doi.org/10.1016/j.neures.2023.07.003>
- Basso, M. A., Bickford, M. E., & Cang, J. (2021). Unraveling circuits of visual perception and cognition through the superior colliculus. *Neuron*, 109(6), 918–937. <https://doi.org/10.1016/j.neuron.2021.01.013>
- Beier, K. T., Steinberg, E. E., DeLoach, K. E., Xie, S., Miyamichi, K., Schwarz, L., Gao, X. J., Kremer, E. J., Malenka, R. C., & Luo, L. (2015). Circuit Architecture of VTA Dopamine Neurons Revealed by Systematic Input–Output Mapping. *Cell*, 162(3), 622–634. <https://doi.org/10.1016/j.cell.2015.07.015>
- Bellone, C., Contestabile, A., Kojovic, N., Casarotto, G., Delvari, F., Hagmann, P., & Schaefer, Marie. (2024). Translation-Research Approach to Social Orienting Deficits in Autism: The Role of Superior Colliculus-Ventral Tegmental Pathway. <https://doi.org/10.21203/rs.3.rs-4017167/v1>
- Berke, J. D. (2018). What does dopamine mean? *Nature Neuroscience*, 21(6), 787–793. <https://doi.org/10.1038/s41593-018-0152-y>
- Berridge, K. C., & Robinson, T. E. (1998). What is the role of dopamine in reward: Hedonic impact, reward learning, or incentive salience? *Brain Research Reviews*, 28(3), 309–369. [https://doi.org/10.1016/S0165-0173\(98\)00019-8](https://doi.org/10.1016/S0165-0173(98)00019-8)
- Bertram, C., Dahan, L., Boorman, L. W., Harris, S., Vautrelle, N., Lerche, M., Redgrave, P., & Overton, P. G. (2014). Cortical regulation of dopaminergic neurons: Role of the midbrain superior colliculus. *Journal of Neurophysiology*, 111(4), 755–767. <https://doi.org/10.1152/jn.00329.2013>
- Boughter, J. D., Lu, L., Saites, L. N., & Tokita, K. (2019). Sweet and bitter taste stimuli activate VTA projection neurons in the parabrachial nucleus. *Brain Research*, 1714, 99–110. <https://doi.org/10.1016/j.brainres.2019.02.027>
- Bromberg-Martin, E. S., Matsumoto, M., & Hikosaka, O. (2010a). Dopamine in Motivational Control: Rewarding, Aversive, and Alerting. *Neuron*, 68(5), 815–834. <https://doi.org/10.1016/j.neuron.2010.11.022>
- Bromberg-Martin, E. S., Matsumoto, M., & Hikosaka, O. (2010b). Dopamine in motivational control: Rewarding, aversive, and alerting. *Neuron*, 68(5), 815–834. <https://doi.org/10.1016/j.neuron.2010.11.022>
- Chevalier, G., & Deniau, J. M. (1984). Spatio-temporal organization of a branched tecto-spinal/tecto-diencephalic neuronal system. *Neuroscience*, 12(2), 427–439. [https://doi.org/10.1016/0306-4522\(84\)90063-0](https://doi.org/10.1016/0306-4522(84)90063-0)
- Coizet, V., Comoli, E., Westby, G. W. M., & Redgrave, P. (2003). Phasic activation of substantia nigra and the ventral tegmental area by chemical stimulation of the superior colliculus: An electrophysiological investigation in the rat. *European Journal of Neuroscience*, 17(1), 28–40. <https://doi.org/10.1046/j.1460-9568.2003.02415.x>
- Coizet, V., Overton, P. G., & Redgrave, P. (2007). Collateralization of the tectonigral projection with other major output pathways of superior colliculus in the rat. *Journal of Comparative Neurology*, 500(6), 1034–1049. <https://doi.org/10.1002/cne.21202>
- Collins, A. L., & Saunders, B. T. (2020). Heterogeneity in striatal dopamine circuits: Form and function in dynamic reward seeking. *Journal of Neuroscience Research*, 98(6), 1046–1069. <https://doi.org/10.1002/jnr.24587>
- Comoli, E., Coizet, V., Boyes, J., Bolam, J. P., Canteras, N. S., Quirk, R. H., Overton, P. G., & Redgrave, P. (2003). A direct projection from superior colliculus to substantia nigra for detecting salient visual events. *Nature Neuroscience*, 6(9), 974. <https://doi.org/10.1038/nn1113>
- Cooper, B. g., Miya, D. y., & Mizumori, S. j. y. (1998). Superior colliculus and active navigation: Role of visual and non-visual cues in controlling cellular representations of space. *Hippocampus*, 8(4), 340–372. [https://doi.org/10.1002/\(SICI\)1098-1063\(1998\)8:4<340::AID-HIPO4>3.0.CO;2-L](https://doi.org/10.1002/(SICI)1098-1063(1998)8:4<340::AID-HIPO4>3.0.CO;2-L)

- Cover, K. K., Elliott, K., Preuss, S. M., & Krauzlis, R. J. (2024). A distinct circuit for biasing visual perceptual decisions and modulating superior colliculus activity through the mouse posterior striatum (p. 2024.07.31.605853). bioRxiv. <https://doi.org/10.1101/2024.07.31.605853>
- Cragg, S., Rice, M. E., & Greenfield, S. A. (1997). Heterogeneity of electrically evoked dopamine release and reuptake in substantia nigra, ventral tegmental area, and striatum. *Journal of Neurophysiology*, 77(2), 863–873. <https://doi.org/10.1152/jn.1997.77.2.863>
- Clegg, J. M., Leiras, R., Montalant, A., Wanken, P., Wickershaw, I. R., & Kiehn, O. (2020). Brainstem neurons that command mammalian locomotor asymmetries. *Nature Neuroscience*, 23(6), Article 6. <https://doi.org/10.1038/s41593-020-0633-7>
- da Silva, J. A., Tecuapetla, F., Paixão, V., & Costa, R. M. (2018). Dopamine neuron activity before action initiation gates and invigorates future movements. *Nature*, 554(7691), 244–248. <https://doi.org/10.1038/nature25457>
- Dawbarn, D., & Pycock, C. J. (1982). Lesions of the superior colliculus in the rat differentiate between nigrostriatal and mesolimbic dopamine systems. *Brain Research*, 235(1), 148–155. [https://doi.org/10.1016/0006-8993\(82\)90205-0](https://doi.org/10.1016/0006-8993(82)90205-0)
- de Araujo, M. F. P., Matsumoto, J., Ono, T., & Nishijo, H. (2015). An animal model of disengagement: Temporary inactivation of the superior colliculus impairs attention disengagement in rats. *Behavioural Brain Research*, 293, 34–40. <https://doi.org/10.1016/j.bbr.2015.07.031>
- Dean, P., Redgrave, P., & Westby, G. W. (1989). Event or emergency? Two response systems in the mammalian superior colliculus. *Trends in Neurosciences*, 12(4), 137–147. [https://doi.org/10.1016/0166-2236\(89\)90052-0](https://doi.org/10.1016/0166-2236(89)90052-0)
- Dommett, E., Coizet, V., Blaha, C. D., Martindale, J., Lefebvre, V., Walton, N., Mayhew, J. E. W., Overton, P. G., & Redgrave, P. (2005). How Visual Stimuli Activate Dopaminergic Neurons at Short Latency. *Science*, 307(5714), 1476–1479. <https://doi.org/10.1126/science.1107026>
- Engel, L., Wolff, A. R., Blake, M., Collins, V. L., Sinha, S., & Saunders, B. T. (2024). Dopamine neurons drive spatio-temporally heterogeneous striatal dopamine signals during learning. *Current Biology*, 34(14), 3086-3101.e4. <https://doi.org/10.1016/j.cub.2024.05.069>
- Engelhard, B., Finkelstein, J., Cox, J., Fleming, W., Jang, H. J., Ornelas, S., Koay, S. A., Thibierge, S. Y., Daw, N. D., Tank, D. W., & Witten, I. B. (2019). Specialized coding of sensory, motor and cognitive variables in VTA dopamine neurons. *Nature*, 570(7762), 509–513. <https://doi.org/10.1038/s41586-019-1261-9>
- Evans, D. A., Stempel, A. V., Vale, R., Ruehle, S., Lefler, Y., & Branco, T. (2018). A synaptic threshold mechanism for computing escape decisions. *Nature*, 558(7711), 590–594. <https://doi.org/10.1038/s41586-018-0244-6>
- Farassat, N., Costa, K. M., Stojanovic, S., Albert, S., Koacheva, L., Shin, J., Egger, R., Somayaji, M., Duvarci, S., Schneider, G., & Roeper, J. (2019). In vivo functional diversity of midbrain dopamine neurons within identified axonal projections. *eLife*, 8, e48408. <https://doi.org/10.7554/eLife.48408>
- Ferguson, S., Eskenazi, D., Ishikawa, M., Wanat, M., Phillips, P., Dong, Y., Roth, B., & Neumaier, J. (2011). Transient neuronal inhibition reveals opposing roles of indirect and direct pathways in sensitization. *Nature Neuroscience*, 14(1), 22–24. <https://doi.org/10.1038/nn.2703>
- Fischbach, S., & Janak, P. H. (2019). Decreases in Cued Reward Seeking After Reward-Paired Inhibition of Mesolimbic Dopamine. *Neuroscience*, 412, 259–269. <https://doi.org/10.1016/j.neuroscience.2019.04.035>
- Fraser, K. M., Pribut, H. J., Janak, P. H., & Keiflin, R. (2023). From Prediction to Action: Dissociable Roles of Ventral Tegmental Area and Substantia Nigra Dopamine Neurons in Instrumental Reinforcement. *The Journal of Neuroscience*, 43(21), 3895–3908. <https://doi.org/10.1523/JNEUROSCI.0028-23.2023>
- Goldberg, M. E., & Wurtz, R. H. (1972). Activity of superior colliculus in behaving monkey. II. Effect of attention on neuronal responses. *Journal of Neurophysiology*, 35(4), 560–574. <https://doi.org/10.1152/jn.1972.35.4.560>
- Grace, A. A., Floresco, S. B., Goto, Y., & Lodge, D. J. (2007). Regulation of firing of dopaminergic neurons and control of goal-directed behaviors. *Trends in Neurosciences*, 30(5), 220–227. <https://doi.org/10.1016/j.tins.2007.03.003>
- Handler, A., Graham, T. G. W., Cohn, R., Morantte, I., Siliciano, A. F., Zeng, J., Li, Y., & Ruta, V. (2019). Distinct dopamine receptor pathways underlie the temporal sensitivity of associative learning. *Cell*, 178(1), 60-75.e19. <https://doi.org/10.1016/j.cell.2019.05.040>
- Hopp, J. J., & Fuchs, A. F. (2004). The characteristics and neuronal substrate of saccadic eye movement plasticity. *Progress in Neurobiology*, 72(1), 27–53. <https://doi.org/10.1016/j.pneurobio.2003.12.002>
- Howe, M., & Dombeck, D. (2016). Rapid signaling in distinct dopaminergic axons during locomotion and reward. *Nature*, 535(7613), 505–510. <https://doi.org/10.1038/nature18942>
- Hoy, J. L., Bishop, H. I., & Niell, C. M. (2019). Defined cell types in superior colliculus make distinct contributions to prey capture behavior in the mouse. *bioRxiv*, 626622. <https://doi.org/10.1101/626622>
- Huang, M., Li, D., Cheng, X., Pei, Q., Xie, Z., Gu, H., Zhang, X., Chen, Z., Liu, A., Wang, Y., Sun, F., Li, Y., Zhang, J., He, M., Xie, Y., Zhang, F., Qi, X., Shang, C., & Cao, P. (2021). The tectonigral pathway regulates appetitive locomotion in predatory hunting in mice. *Nature Communications*, 12(1), 4409. <https://doi.org/10.1038/s41467-021-24696-3>
- Hughes RN, Bakhurin KI, Petter EA, Watson GDR, Kim N, Friedman AD, Yin HH (2020) Ventral Tegmental Dopamine Neurons Control the Impulse Vector during Motivated Behavior. *Curr Biol* 30:2681-2694.e5.

- Ignashchenkova, A., Dicke, P. W., Haarmeier, T., & Thier, P. (2004). Neuron-specific contribution of the superior colliculus to overt and covert shifts of attention. *Nature Neuroscience*, 7(1), 56–64. <https://doi.org/10.1038/nn1169>
- Ikeda, T., & Hikosaka, O. (2007). Positive and Negative Modulation of Motor Response in Primate Superior Colliculus by Reward Expectation. *Journal of Neurophysiology*, 98(6), 3163–3170. <https://doi.org/10.1152/jn.00975.2007>
- Ikemoto, S. (2007). Dopamine reward circuitry: Two projection systems from the ventral midbrain to the nucleus accumbens-olfactory tubercle complex. *Brain Research Reviews*, 56(1), 27–78. <https://doi.org/10.1016/j.brainresrev.2007.05.004>
- Ilanga, A., Kesner, A. J., Keller, K. L., Stuber, G. D., Bonci, A., & Ikemoto, S. (2014). Similar Roles of Substantia Nigra and Ventral Tegmental Dopamine Neurons in Reward and Aversion. *The Journal of Neuroscience*, 34(3), 817–822. <https://doi.org/10.1523/JNEUROSCI.1703-13.2014>
- Isa, K., Sookswate, T., Kobayashi, K., Kobayashi, K., Redgrave, P., & Isa, T. (2019). Difference in context-dependency between orienting and defense-like responses induced by the superior colliculus [Preprint]. *Neuroscience*. <https://doi.org/10.1101/729772>
- Ito, S., & Feldheim, D. A. (2018). The Mouse Superior Colliculus: An Emerging Model for Studying Circuit Formation and Function. *Frontiers in Neural Circuits*, 12. <https://doi.org/10.3389/fncir.2018.00010>
- Kaźmierczak, M., & Nicola, S. M. (2022). The arousal-motor hypothesis of dopamine function: Evidence that dopamine facilitates reward seeking in part by maintaining arousal. *Neuroscience*, 499, 64–103. <https://doi.org/10.1016/j.neuroscience.2022.07.008>
- Keiflin, R., Pribut, Heather. J., Shah, N. B., & Janak, P. H. (2019). Ventral Tegmental Dopamine Neurons Participate in Reward Identity Predictions. *Current Biology : CB*, 29(1), 93–103.e3. <https://doi.org/10.1016/j.cub.2018.11.050>
- Kim, C. K., Yang, S. J., Pichamoothy, N., Young, N. P., Kauvar, I., Jennings, J. H., Lerner, T. N., Berndt, A., Lee, S. Y., Ramakrishnan, C., Davidson, T. J., Inoue, M., Bito, H., & Deisseroth, K. (2016). Simultaneous fast measurement of circuit dynamics at multiple sites across the mammalian brain. *Nature Methods*, 13(4), Article 4. <https://doi.org/10.1038/nmeth.3770>
- Klapoetke, N. C., Murata, Y., Kim, S. S., Pulver, S. R., Birdsey-Benson, A., Cho, Y. K., Morimoto, T. K., Chuong, A. S., Carpenter, E. J., Tian, Z., Wang, J., Xie, Y., Yan, Z., Zhang, Y., Chow, B. Y., Surek, B., Melkonian, M., Jayaraman, V., Constantine-Paton, M., ... Boyden, E. S. (2014). Independent Optical Excitation of Distinct Neural Populations. *Nature Methods*, 11(3), 338–346. <https://doi.org/10.1038/nmeth.2836>
- Krauzlis, R. J., Lovejoy, L. P., & Zénon, A. (2013). Superior Colliculus and Visual Spatial Attention. *Annual Review of Neuroscience*, 36. <https://doi.org/10.1146/annurev-neu-051012-150249>
- Kravitz, A. V., Freeze, B. S., Parker, P. R. L., Kay, K., Thwin, M. T., Deisseroth, K., & Kreitzer, A. C. (2010). Regulation of parkinsonian motor behaviors by optogenetic control of basal ganglia circuitry. *Nature*, 466(7306), 622–626. <https://doi.org/10.1038/nature09159>
- Lak A, Okun M, Moss MM, Gurnani H, Farrell K, Wells MJ, Reddy CB, Kepcs A, Harris KD, Carandini M (2020) Dopaminergic and Prefrontal Basis of Learning from Sensory Confidence and Reward Value. *Neuron* 105:700-711.e6.
- Lammel, S., Hetzel, A., Häckel, O., Jones, I., Liss, B., & Roepke, J. (2008). Unique properties of mesoprefrontal neurons within a dual mesocorticolimbic dopamine system. *Neuron*, 57(5), 760–773. <https://doi.org/10.1016/j.neuron.2008.01.022>
- Lee, J., & Sabatini, B. L. (2021). Striatal indirect pathway mediates exploration via collicular competition. *Nature*, 599(7886), 645–649. <https://doi.org/10.1038/s41586-021-04055-4>
- Lee, J., Wang, W., & Sabatini, B. L. (2020). Anatomically segregated basal ganglia pathways allow parallel behavioral modulation. *Nature Neuroscience*, 23(11), 1388–1398. <https://doi.org/10.1038/s41593-020-00712-5>
- Lerner, T. N., Holloway, A. L., & Seiler, J. L. (2021). Dopamine, Updated: Reward Prediction Error and Beyond. *Current Opinion in Neurobiology*, 67, 123–130. <https://doi.org/10.1016/j.conb.2020.10.012>
- Lerner, T. N., Shilyansky, C., Davidson, T. J., Evans, K. E., Beier, K. T., Zalocusky, K. A., Crow, A. K., Malenka, R. C., Luo, L., Tomer, R., & Deisseroth, K. (2015). Intact-Brain Analyses Reveal Distinct Information Carried by SNc Dopamine Subcircuits. *Cell*, 162(3), 635–647. <https://doi.org/10.1016/j.cell.2015.07.014>
- Lobo, M. K., Covington, H. E., Chaudhury, D., Friedman, A. K., Sun, H., Damez-Werno, D., Dietz, D. M., Zaman, S., Koo, J. W., Kennedy, P. J., Mouzon, E., Mogri, M., Neve, R. L., Deisseroth, K., Han, M.-H., & Nestler, E. J. (2010). Cell type-specific loss of BDNF signaling mimics optogenetic control of cocaine reward. *Science (New York, N.Y.)*, 330(6002), 385–390. <https://doi.org/10.1126/science.118472>
- Lovejoy, L. P., & Krauzlis, R. J. (2010). Inactivation of primate superior colliculus impairs covert selection of signals for perceptual judgments. *Nature Neuroscience*, 13(2), 261–266. <https://doi.org/10.1038/nn.2470>
- Magos, L. (1969). Persistence of the effect of amphetamine on stereotyped activity in rats. *European Journal of Pharmacology*, 6(2), 200–201. [https://doi.org/10.1016/0014-2999\(69\)90220-9](https://doi.org/10.1016/0014-2999(69)90220-9)
- Mana, S., & Chevalier, G. (2001). The fine organization of nigro-collicular channels with additional observations of their relationships with acetylcholinesterase in the rat. *Neuroscience*, 106(2), 357–374. [https://doi.org/10.1016/s0306-4522\(01\)00283-4](https://doi.org/10.1016/s0306-4522(01)00283-4)
- Mathis, A., Mamidanna, P., Cury, K. M., Abe, T., Murthy, V.

- N., Mathis, M. W., & Bethge, M. (2018). DeepLabCut: Markerless pose estimation of user-defined body parts with deep learning. *Nature Neuroscience*, 21(9), 1281–1289. <https://doi.org/10.1038/s41593-018-0209-y>
- May, P. J. (2006). The mammalian superior colliculus: Laminar structure and connections. In J. A. Büttner-Ennever (Ed.), *Progress in Brain Research* (Vol. 151, pp. 321–378). Elsevier. [https://doi.org/10.1016/S0079-6123\(05\)51011-2](https://doi.org/10.1016/S0079-6123(05)51011-2)
- May, P. J., McHaffie, J. G., Stanford, T. R., Jiang, H., Costello, M. G., Coizet, V., Hayes, L. M., Haber, S. N., & Redgrave, P. (2009). Tectonigral projections in the primate: A pathway for pre-attentive sensory input to midbrain dopaminergic neurons. *European Journal of Neuroscience*, 29(3), 575–587. <https://doi.org/10.1111/j.1460-9568.2008.06596.x>
- McHaffie, J. G., Jiang, H., May, P. J., Coizet, V., Overton, P. G., Stein, B. E., & Redgrave, P. (2006). A direct projection from superior colliculus to substantia nigra pars compacta in the cat. *Neuroscience*, 138(1), 221–234. <https://doi.org/10.1016/j.neuroscience.2005.11.015>
- Mohebi, A., Pettibone, J. R., Hamid, A. A., Wong, J.-M. T., Vinson, L. T., Patriarchi, T., Tian, L., Kennedy, R. T., & Berke, J. D. (2019). Dissociable dopamine dynamics for learning and motivation. *Nature*, 570(7759), 65–70. <https://doi.org/10.1038/s41586-019-1235-y>
- Mysore, S. P., & Knudsen, E. I. (2011). The role of a midbrain network in competitive stimulus selection. *Current Opinion in Neurobiology*, 21(4), 653–660. <https://doi.org/10.1016/j.conb.2011.05.024>
- Nair-Roberts, R. G., Chatelain-Badie, S. D., Benson, E., White-Cooper, H., Bolam, J. P., & Ungless, M. A. (2008). Stereological estimates of dopaminergic, GABAergic and glutamatergic neurons in the ventral tegmental area, substantia nigra and retrorubral field in the rat. *Neuroscience*, 152(4–2), 1024–1031. <https://doi.org/10.1016/j.neuroscience.2008.01.046>
- Prévost, E. D., Phillips, A., Lauridsen, K., Enserro, G., Rubinstein, B., Alas, D., McGovern, D. J., Ly, A., Hotchkiss, H., Banks, M., McNulty, C., Kim, Y. S., Fenno, L. E., Ramakrishnan, C., Deisseroth, K., & Root, D. H. (2024). Monosynaptic inputs to ventral tegmental area glutamate and GABA co-transmitting neurons. *Journal of Neuroscience*. <https://doi.org/10.1523/JNEUROSCI.2184-23.2024>
- Redgrave, P., Coizet, V., Comoli, E., McHaffie, J. G., Leriche, M., Vautrelle, N., Hayes, L. M., & Overton, P. (2010). Interactions between the Midbrain Superior Colliculus and the Basal Ganglia. *Frontiers in Neuroanatomy*, 4. <https://doi.org/10.3389/fnana.2010.00132>
- Redgrave, P., Coizet, V., Comoli, E., McHaffie, J. G., Leriche, Vazquez, M., Vautrelle, N., Hayes, L. M., & Overton, P. G. (2010). Interactions between the Midbrain Superior Colliculus and the Basal Ganglia. *Frontiers in Neuroanatomy*, 4. <https://doi.org/10.3389/fnana.2010.00132>
- Redgrave, P., & Gurney, K. (2006). The short-latency dopamine signal: A role in discovering novel actions? *Nature Reviews Neuroscience*, 7(12), Article 12. <https://doi.org/10.1038/nrn2022>
- Redgrave, P., Prescott, T. J., & Gurney, K. (1999). Is the short-latency dopamine response too short to signal reward error? *Trends in Neurosciences*, 22(4), 146–151. [https://doi.org/10.1016/s0166-2236\(98\)01373-3](https://doi.org/10.1016/s0166-2236(98)01373-3)
- Sahibzada, N., Dean, P., & Redgrave, P. (1986). Movements resembling orientation or avoidance elicited by electrical stimulation of the superior colliculus in rats. *The Journal of Neuroscience*, 6(3), 723–733. <https://doi.org/10.1523/JNEUROSCI.06-03-00723.1986>
- Saunders, B. T., Richard, J. M., Margolis, E. B., & Janak, P. H. (2018). Dopamine neurons create Pavlovian conditioned stimuli with circuit-defined motivational properties. *Nature Neuroscience*, 21(8), 1072–1083. <https://doi.org/10.1038/s41593-018-0191-4>
- Schultz, W. (1998). Predictive Reward Signal of Dopamine Neurons. *Journal of Neurophysiology*, 80(1), 1–27. <https://doi.org/10.1152/jn.1998.80.1.1>
- Schultz, W. (2007). Multiple Dopamine Functions at Different Time Courses. *Annual Review of Neuroscience*, 30(1), 259–288. <https://doi.org/10.1146/annurev.neuro.28.061604.135722>
- Scott, A., Palmer, D., Newell, B., Lin, I., Cayton, C. A., Paulson, A., Remde, P., & Richard, J. M. (2023). Ventral Pallidal GABAergic Neuron Calcium Activity Encodes Cue-Driven Reward Seeking and Persists in the Absence of Reward Delivery. *Journal of Neuroscience*, 43(28), 5191–5203. <https://doi.org/10.1523/JNEUROSCI.0013-23.2023>
- Sharpe, M. J., Chang, C. Y., Liu, M. A., Batchelor, H. M., Mueller, L. E., Jones, J. L., Niv, Y., & Schoenbaum, G. (2017). Dopamine transients are sufficient and necessary for acquisition of model-based associations. *Nature Neuroscience*, 20(5), 735–742. <https://doi.org/10.1038/nn.4538>
- Solié, C., Contestabile, A., Espinosa, P., Musardo, S., Barisielli, S., Huber, C., Carleton, A., & Bellone, C. (2022). Superior Colliculus to VTA pathway controls orienting response and influences social interaction in mice. *Nature Communications*, 13(1), 817. <https://doi.org/10.1038/s41467-022-28512-4>
- Steinberg, E. E., Boivin, J. R., Saunders, B. T., Witten, I. B., Deisseroth, K., & Janak, P. H. (2014). Positive Reinforcement Mediated by Midbrain Dopamine Neurons Requires D1 and D2 Receptor Activation in the Nucleus Accumbens. *PLoS ONE*, 9(4). <https://doi.org/10.1371/journal.pone.0094771>
- Steinmetz, N. A., Zatka-Haas, P., Carandini, M., & Harris, K. D. (2019). Distributed coding of choice, action and engagement across the mouse brain. *Nature*, 576(7786), 266–273. <https://doi.org/10.1038/s41586-019-1787-x>
- Suzuki, D. G., Pérez-Fernández, J., Wibble, T., Kardamakis, A. A., & Grillner, S. (2019). The role of the optic tectum for visually evoked orienting and evasive movements. *Proceedings of the National Academy of Sciences*, 116(30), 15272–15281. <https://doi.org/10.1073/pnas.1907962116>

- Takakuwa, N., Kato, R., Redgrave, P., & Isa, T. (2017). Emergence of visually-evoked reward expectation signals in dopamine neurons via the superior colliculus in V1 lesioned monkeys. *eLife*, 6, e24459. <https://doi.org/10.7554/eLife.24459>
- Taylor, S. R., Badurek, S., Dileone, R. J., Nashmi, R., Minichiello, L., & Picciotto, M. R. (2014). GABAergic and glutamatergic efferents of the mouse ventral tegmental area. *The Journal of Comparative Neurology*, 522(14), 3308–3334. <https://doi.org/10.1002/cne.23603>
- Thomas, A., Yang, W., Wang, C., Tippuraj, S. L., Chen, G., Sullivan, B., Swiekowski, K., Tatam, M., Gerfen, C., & Li, N. (2023). Superior colliculus bidirectionally modulates choice activity in frontal cortex. *Nature Communications*, 14(1), 7358. <https://doi.org/10.1038/s41467-023-43252-9>
- Tian, J., Huang, R., Cohen, J. Y., Osakada, F., Kobak, D., Machens, C. K., Callaway, E. M., Uchida, N., & Watabe-Uchida, M. (2016). Distributed and Mixed Information in Monosynaptic Inputs to Dopamine Neurons. *Neuron*, 91(6), 1374–1389. <https://doi.org/10.1016/j.neuron.2016.08.018>
- Tsai, H.-C., Zhang, F., Adamantidis, A., Stuber, G. D., Bonci, A., de Lecea, L., & Deisseroth, K. (2009). Phasic Firing in Dopaminergic Neurons Is Sufficient for Behavioral Conditioning. *Science (New York, N.Y.)*, 324(5930), 1080–1084. <https://doi.org/10.1126/science.1168878>
- Ungless, M. A., & Grace, A. A. (2012). Are you or aren't you? Challenges associated with physiologically identifying dopamine neurons. *Trends in Neurosciences*, 35(7), 422–430. <https://doi.org/10.1016/j.tins.2012.02.003>
- van Zessen, R., Flores-Dourojeanni, J. P., Eekel, T., van den Reijen, S., Lodder, B., Omrani, A., Smidt, M. P., Ramakers, G. M. J., van der Plasse, G., Stuber, G. D., & Adan, R. A. H. (2021). Cue and Reward Evoked Dopamine Activity Is Necessary for Maintaining Learned Pavlovian Associations. *The Journal of Neuroscience: The Official Journal of the Society for Neuroscience*, 41(23), 5004–5014. <https://doi.org/10.1523/JNEUROSCI.2744-20.2021>
- Villalobos, C. A., & Basso, M. A. (2020). Optogenetic activation of the inhibitory nigro-collicular circuit evokes orienting movements in mice. *bioRxiv*, 2020.05.21.107680. <https://doi.org/10.1101/2020.05.21.107680>
- Viviani, R., Dommes, L., Bosch, J., Steffens, M., Paul, A., Schneider, K. L., Stingl, J. C., & Beschoner, P. (2020). Signals of anticipation of reward and of mean reward rates in the human brain. *Scientific Reports*, 10(1), Article 1. <https://doi.org/10.1038/s41598-020-61257-y>
- Wakabayashi, K. T., Feja, M., Baird, A. N., Bruno, M. J., Bhimani, R. V., Park, J., Hausknecht, K., Shen, R.-Y., Haj-Dahmane, S., & Bass, C. E. (2019). Chemogenetic activation of ventral tegmental area GABA neurons, but not mesoaccumbal GABA terminals, disrupts responding to reward-predictive cues. *Neuropsychopharmacology: Official Publication of the American College of Neuropsychopharmacology*, 44(2), 372–380. <https://doi.org/10.1038/s41386-018-0097-6>
- Wang, L., McAlonan, K., Goldstein, S., Gerfen, C. R., & Kraus, R. J. (2020). A Causal Role for Mouse Superior Colliculus in Visual Perceptual Decision-Making. *The Journal of Neuroscience*, 40(19), 3768–3782. <https://doi.org/10.1523/JNEUROSCI.2642-19.2020>
- Watabe-Uchida, M., Zhu, L., Ogawa, S. K., Vamanrao, A., & Uchida, N. (2012). Whole-Brain Mapping of Direct Inputs to Midbrain Dopamine Neurons. *Neuron*, 74(5), 858–873. <https://doi.org/10.1016/j.neuron.2012.03.017>
- White, B. J., Kan, J. Y., Levy, R., Itti, L., & Munoz, D. P. (2017). Superior colliculus encodes visual saliency before the primary visual cortex. *Proceedings of the National Academy of Sciences*, 114(35), 9451–9456. <https://doi.org/10.1073/pnas.1701003114>
- White, B. J., & Munoz, D. P. (2011). Separate Visual Signals for Saccade Initiation during Target Selection in the Primate Superior Colliculus. *Journal of Neuroscience*, 31(5), 1570–1578. <https://doi.org/10.1523/JNEUROSCI.5349-10.2011>
- Wise, R. A. (2009). Roles for nigrostriatal—Not just mesocorticolimbic—Dopamine in reward and addiction. *Trends in Neurosciences*, 32(10), 517–524. <https://doi.org/10.1016/j.tins.2009.06.004>
- Wise, R. A., & Jordan, C. J. (2021). Dopamine, behavior, and addiction. *Journal of Biomedical Science*, 28(1), 83. <https://doi.org/10.1186/s12929-021-00779-7>
- Wise, R. A., & Robble, M. A. (2020). Dopamine and Addiction. *Annual Review of Psychology*, 71, 79–106. <https://doi.org/10.1146/annurev-psych-010418-103337>
- Witten, I. B., Steinberg, E. E., Lee, S. Y., Davidson, T. J., Zalcusky, K. A., Brodsky, M., Yizhar, O., Cho, S. L., Gong, S., Ramakrishnan, C., Stuber, G. D., Tye, K. M., Janak, P. H., & Deisseroth, K. (2011). Recombinase-driver rat lines: Tools, techniques, and optogenetic application to dopamine-mediated reinforcement. *Neuron*, 72(5), 721–733. <https://doi.org/10.1016/j.neuron.2011.10.028>
- Yoshida, M., Itti, L., Berg, D. J., Ikeda, T., Kato, R., Takaura, K., White, B. J., Munoz, D. P., & Isa, T. (2012). Residual attention guidance in blindsight monkeys watching complex natural scenes. *Current Biology: CB*, 22(15), 1429–1434. <https://doi.org/10.1016/j.cub.2012.05.046>
- Zhang, Y., Rózsa, M., Liang, Y., Bushey, D., Wei, Z., Zheng, J., Reep, D., Broussard, G. J., Tsang, A., Tsegaye, G., Narayan, S., Obara, C. J., Lim, J.-X., Patel, R., Zhang, R., Ahrens, M. B., Turner, G. C., Wang, S. S.-H., Korff, W. L., ... Looger, L. L. (2023). Fast and sensitive GCAMP calcium indicators for imaging neural populations. *Nature*, 615(7954), Article 7954. <https://doi.org/10.1038/s41586-023-05828-9>
- Zhou, W.-L., Kim, K., Ali, F., Pittenger, S. T., Calarco, C. A., Mineur, Y. S., Ramakrishnan, C., Deisseroth, K., Kwan, A. C., & Picciotto, M. R. (2022). Activity of a direct VTA to ventral pallidum GABA pathway encodes unconditioned reward value and sustains motivation for reward. *Science Advances*, 8(42), eabm5217. <https://doi.org/10.1126/sciadv.abm5217>
- Zhou, Z., Liu, X., Chen, S., Zhang, Z., Liu, Y., Montardy, Q., Poisson et al. Superior colliculus activates dopamine neurons for movement not value

Tang, Y., Wei, P., Liu, N., Li, L., Song, R., Lai, J., He, X., Chen, C., Bi, G., Feng, G., Xu, F., & Wang, L. (2019). A VTA GABAergic Neural Circuit Mediates Visually Evoked Innate Defensive Responses. *Neuron*, 103(3), 473-488.e6. <https://doi.org/10.1016/j.neuron.2019.05.027>

Zingg, B., Chou, X.-L., Zhang, Z.-G., Mesik, L., Liang, F., Tao, H. W., & Zhang, L. I. (2017). AAV-Mediated Anterograde Transsynaptic Tagging: Mapping Corticocollicular Input-Defined Neural Pathways for Defense Behaviors. *Neuron*, 93(1), 33–47. <https://doi.org/10.1016/j.neuron.2016.11.045>